Synthesis of chemical tools to study the immune system

Graaff, M.J. van de

Chapter 4

Photo-activatable TLR-ligands[1]

Introduction

The *ortho*-nitrobenzyl group (oNB) was reported as a photo-labile protecting group for use in organic synthesis in 1966[2]. Its discovery has since spawned a large body of literature on the use of light-sensitive protecting groups in organic synthesis[3–6]. Initially, the oNB group (Scheme **1**) was used as an ester-protecting group that could be removed with 350-380 nm light.[2] The mechanism leading to liberation of the carboxylic acid is thought to be as follows.[6] Upon irradiation, an excited singlet state is generated, which quickly crosses to an excited triplet state. From this triplet state, a hydrogen atom is abstracted from the benzylic carbon by the nitro-group. The radical species rearranges to form the *aci*-nitro intermediate. This intermediate then forms a 5-membered ketal ring, which collapses to form the nitroso product and the liberated carboxylic acid.
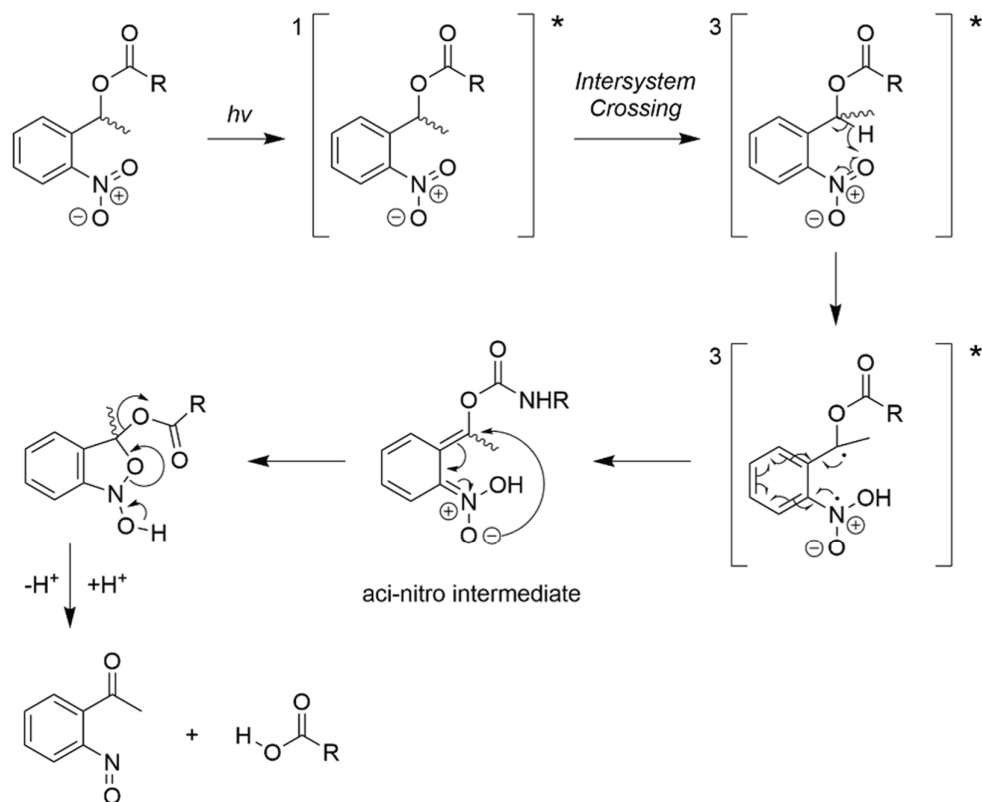
Scheme 1. Deprotection mechanism of benzylic-substituted 2-nitrobenzyls.[6]
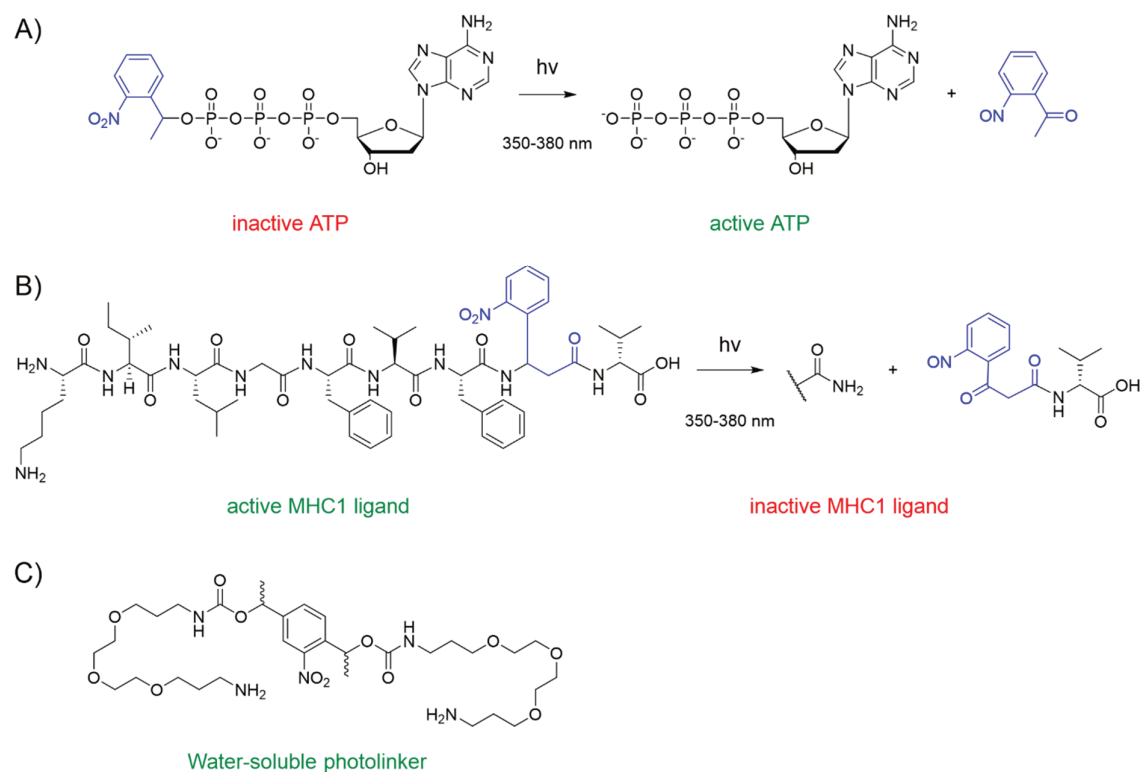
The oNB is able to release a wide varieties on functionalities upon UV-irradiation, including alcohols[7], amines[8], amides[8], carbamates[7], carboxylic acids[2], phosphates[9] and carbonic acids[7]. The oNB protecting group can be used orthogonally with various other protecting groups and has been used in the synthesis of many organic compounds.[4,10]

This orthogonality was picked up quickly by biochemists in 1977[9,11], as it was postulated that this orthogonality to a wide range of chemistries could translate to bioorthogonality of the deprotection reaction. In cells, this is a major issue, due to the wide variety of chemical functionalities present in biological samples that make selective chemistry very difficult.[12] In 1977, Engels[11] and Hoffman[9] found that the oNB-group could be used in this context as well. They reported the light-induced activation of oNB-protected adenosine triphosphate (Scheme **2**A). In these experiments the oNB was used to 'mask'

or 'cage' the activity of a biologically active species. The strategy therefore became known as 'photocaging'[13]. Since these initial experiments, photocages have been used extensively in biology (reviewed here[14]), and various different chemistries have been developed to do so. Coumarin-4-ylmethyl[15]-, BODIPY[16]-, arylcarbonylmethyl[17]- and metal[18]-based structures have all been employed to this end (see also Chapter **1**). These photocages have been used to study a vast array of biological processes, and that involve the (un)caging of a range of metabolites[19], carbohydrates[20], proteins[21], (oligo-)nucleotides,[22,23] peptides[24], and other (small) molecules.[25] In all these examples the photocage was used to mask a biologically active agent that was unmasked upon irradiation with light of a specific wavelength.

In recent years, photocages have also been adapted to achieve the opposite to activating: terminating the biological activity of a molecule upon irradiation. This concept was, for example, exploited to generate empty MHC class I molecules.[8] MHC class I is an unstable complex by itself, but is stabilized by the presence of a peptide with the right size and amino acid composition. A peptide that included a photocage within the amino acid sequence was used to generate stable MHC-peptide complexes (Scheme **2**B). UV irradiation of these complexes bearing the depicted nonapeptide led to dissociation of the resulting heptapeptide, due to the strict length requirements for the peptide ligands. This enabled to loading of epitopes of choice in a high-throughput manner on MHC class I molecules.

Photocages with one photolabile and one or more photo-stabile connections (photolinkers) not only find their use in creating a fissile feature in a biomolecule to silence biological activity upon irradiation, but can also temporarily introduce features into a molecule. For example, the use of a PEG-modified nitrobenzyl-cage was used to enhance the aqueous-solubility of the photocage, to enable its application in affinity supports in proteomics (Scheme **2**C).[26]

A)

inactive ATP   active ATP

B)

active MHC1 ligand   inactive MHC1 ligand

C)

Water-soluble photolinker

Scheme 2. First examples of a nitrobenzyl being employed in a biological system as a photocage (A)[9] and photolinker (B).[8] One of the first reported examples of a solubilized version of a nitrobenzyl photolinker (C).

Despite the numerous applications, the oNB group has some intrinsic shortcomings. The first of these is that its excitation wavelength is in the UV-range (350-380 nm).[7] This part of the electromagnetic spectrum is toxic to most living cells, as nucleobases and certain amino acids can absorb these wavelengths to form reactive species, leading to, for instance, DNA damage.[27] Secondly, the absorbance – the efficiency with which the oNB absorbs photons – is quite low. This efficiency is intrinsic to each photocage and can be described as the molar attenuation coefficient, ε, and is usually given at the wavelength at which the system absorbs the most light, λ_{max}. Given the concentration of the photocage, c, and the pathlength of light, l, the amount of light absorbed in a solution, A, is described by the Lambert-Beer law as $A = \varepsilon * c * l$. From this equation it follows that the amount of light absorbed is linearly correlated to the ε, which for oNB-based photocages is low. The final problem with the oNB-group relates to the spatial resolution with which a sample can be deprotected, making it sub-optimal to investigate biological processes such as TLR-signaling.[28] This is in part due to the Abbe-limit of detection that is intrinsic to the wavelength of light used for the deprotection.[29]

The shortcomings described above have in part been addressed by making analogues of oNB that contain the orthonitrophenyl-group in, for example, an extended conjugated system (Figure **1**, NDBF, NPBF). This modification yielded photocages with increased ε-value compared to the parent-oNB group, and show uncaging with the decreased photo-toxic irradiation of up to 420 nm.[1] Further extension of the aromatic system, and the inclusion of a second nitrobenzyl-group,

yielded the bisstyrylthiophene group with the λ_{max} shifted to 440 nm and a *ε-value* of 250 times higher than oNB.
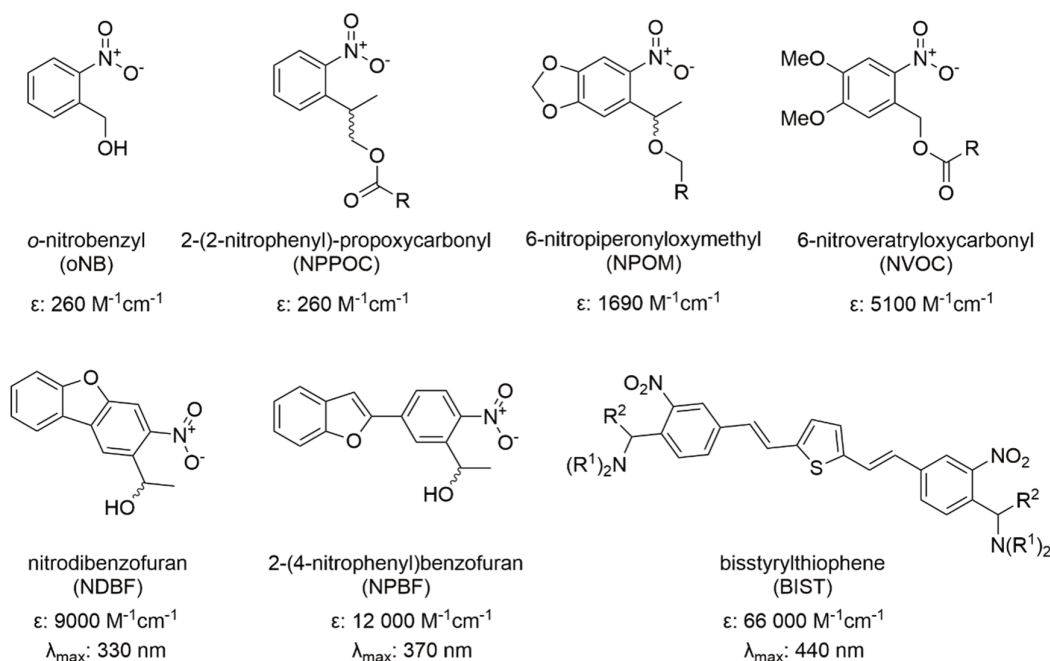

Figure 1. Several derivatives of the oNB-photocage. The NPPOC group has a similar ε-value as the oNB group, but has faster uncaging kinetics[30]. The NPOM-group was developed by the group of Deiters to cage aromatic N-heterocycles which otherwise would hydrolyze quickly in an aqueous pH=7.5 environment[31]. The NVOC-group already has a significant higher absorption coefficient than the oNB-cage[32] and has therefore been employed extensively. The NDBF-group has a much-improved ε-value and its quantum yield of photolysis is 0.7[33], and was thus useable to study cardiac muscle contraction using 2PE. The NPBF-group was synthesized later as an iteration on the NDBF-group to improve its use in 2-photon absorption[34] even further. BIST is a very efficient absorber of light and due to its extended conjugated system it can be cleaved using blue or violet light. It is currently the most-sensitive o-nitrobenzyl-based photocage for single and two-photon uncaging.

These approaches in part solved the issues with wavelength and non-wavelength dependent phototoxicity. They did not, however, address the problem of low uncaging resolution. This can be addressed by using photocages that are sensitive to 2-photon excitation (2PE). In such a 2PE phenomenon, a fluorophore/photocage is excited not by one photon of a given wavelength, but by two photons of double the wavelength. For example, instead of using 1 photon of 350 nm to excite a molecule, 2 photons of 700 nm are absorbed (as energy scales linearly with wavelength according to E= h*c/λ). This requires however an extremely high photon density, as the likelihood of two absorption events to occur simultaneously is very low. Such a high photon density necessitates the use of non-phototoxic wavelengths in the (near-)infrared.
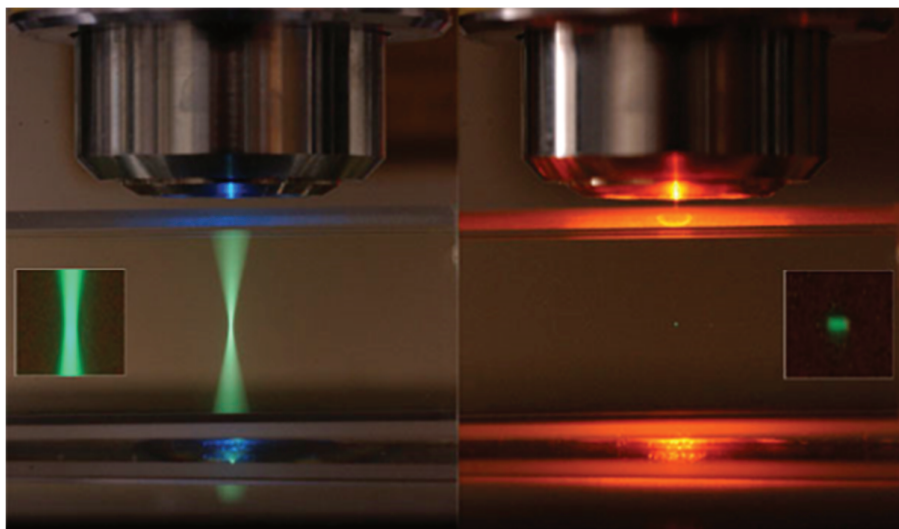
Figure 2. Signal-versus-noise when using single-photon excitation (left-hand side) and two-photon excitation (right hand side). Excitation outside the focal point is much more prominent in single-photon excitation, leading to loss of accuracy when investigating signal-sensitive systems.

Because of the use of lower energetic wavelengths phototoxicity is limited, and tissue penetration is enhanced.[35] The main advantage of 2PE is the high spatial resolution that can be obtained (Figure **2**). Long wavelengths scatter less and two-photon absorption is extremely unlikely outside the focal point, thus reducing the background signal when compared to single-photon excitation. These effects enable the irradiation of single cells and even volumes in the femtoliter range (which would correspond to the volume of single endosomes).[36,37]

In one-photon excitation, the probability of photon absorption is linearly proportional to the light intensity. But in 2PE, two photons are required to be simultaneously absorbed and thus the probability of this absorption process is proportional to the square of the light intensity.[38] For example in 1PE, the portion of caged biomolecules outside the focal point receiving *half* the amount of photons as those in the focal point are uncaged at *half* the rate. But in 2PE, caged biomolecules outside the focal point receiving *half* the amount of photons are uncaged at a *quarter* of the rate. Uncaging outside the region of interest therefore exponentially drops as the distance from the focal point increases. 2PE-uncaging may therefore assist in the unraveling of spatial-dependent signaling events exhibited by the TLR-system.

In this Chapter, the synthesis of 1P- and 2P-sensitive TLR-ligands is described. The oNB-cage and the NPBF-cage were introduced onto TLR-ligands to control their biological activity (Figure **3**). Firstly, a TLR 7 ligand was protected with the 1P-sensitive NVOC (Figure **3**, compound **4**). A solubilized analogue was also made (Figure **3**, compound **3**). TLR2/6 ligands bearing the NPBF-photocage on the N-terminal amine were also synthesized and evaluated (Figure **3**, **1** and **2**).
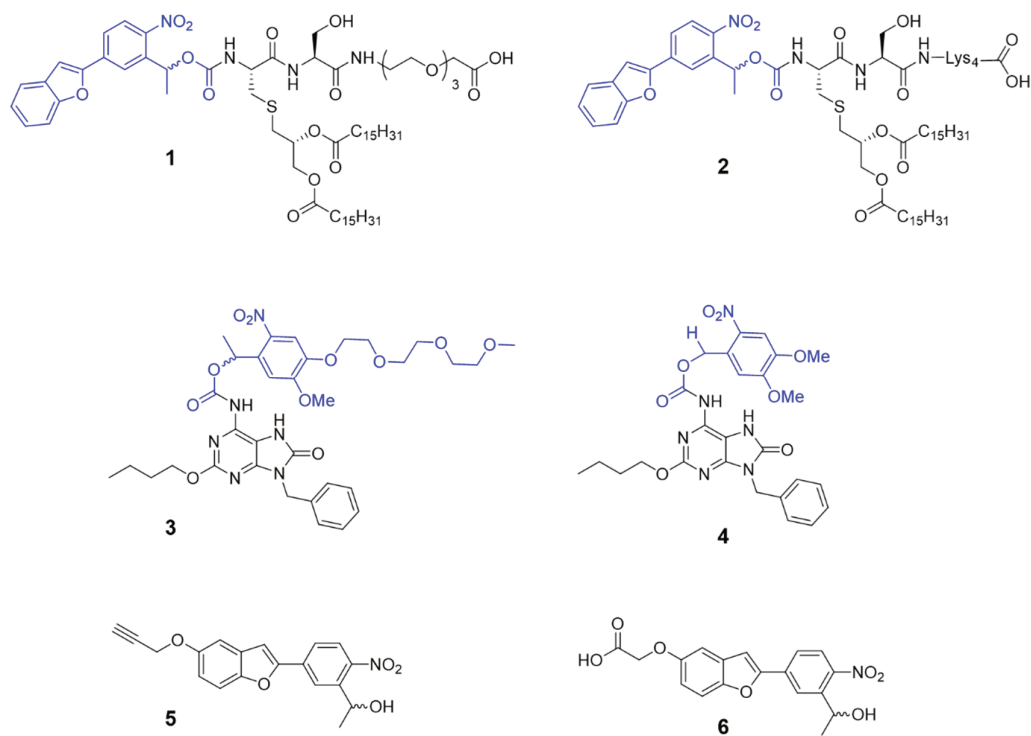
Figure 3. Target compounds described in this Chapter. For compounds **1-4**, photocages are depicted in blue whereas the TLR-ligands are depicted in black. Compounds **5** and **6** are bis-functionalized derivatives of the NPBF photocage.

Results and discussion

Photocaged TLR7 ligands

9-benzyl-8-oxo-2-butoxyadenine (Scheme **3**, compound **7**) is a potent TLR7 agonist (see also Chapter 3)[39] of which the activity can be blocked by protecting the exocyclic amine. A photocaged variant was made by reacting **7** with 6-nitroveratryloxycarbonyl (NVOC)-chloroformate (Scheme **3**).
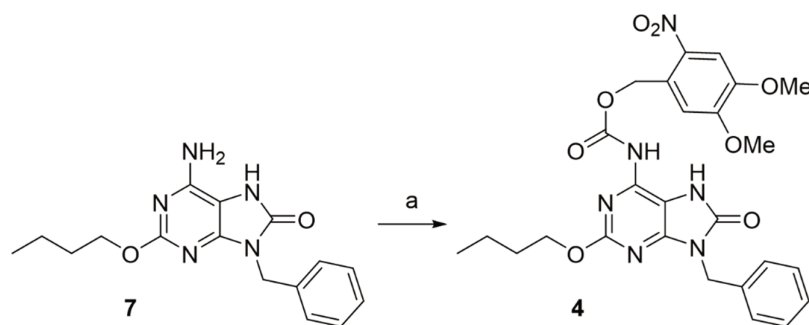
Scheme 3. a) NVOC-Cl, DMAP, dioxane, 50°C, o.n., 19%

Unfortunately, compound **4** was insoluble in aqueous and cell growth media (dilution of the DMSO stock resulted in precipitation in these solvents). It was hypothesized to occur due to the hydrophobic nature of both the TLR-ligand and the photocage. It was therefore opted to use a photo-destructible linker and use the second functionality within the cage to introduce moieties that improve aqueous solubility. A variant of the NVOC-photocage was synthesized in which triethylene glycol was appended to the nitrobenzene photocage (**12**, Scheme **4**), using an intermediate described by Teague et al.[40] 6-Nitropiperonal was first reacted with the nucleophilic methylation reagent trimethyl aluminum, resulting in a racemic mixture of compound **9**. Then a regioselective nucleophilic aromatic displacement with sodium methoxide was carried out affording compound **10**. The phenol functionality could be selectively reacted over the benzylic alcohol under under mildly basic conditions with the mesylate of triethyleneglycol monomethylether (**14**) to yield the solubilized photocage **11**.
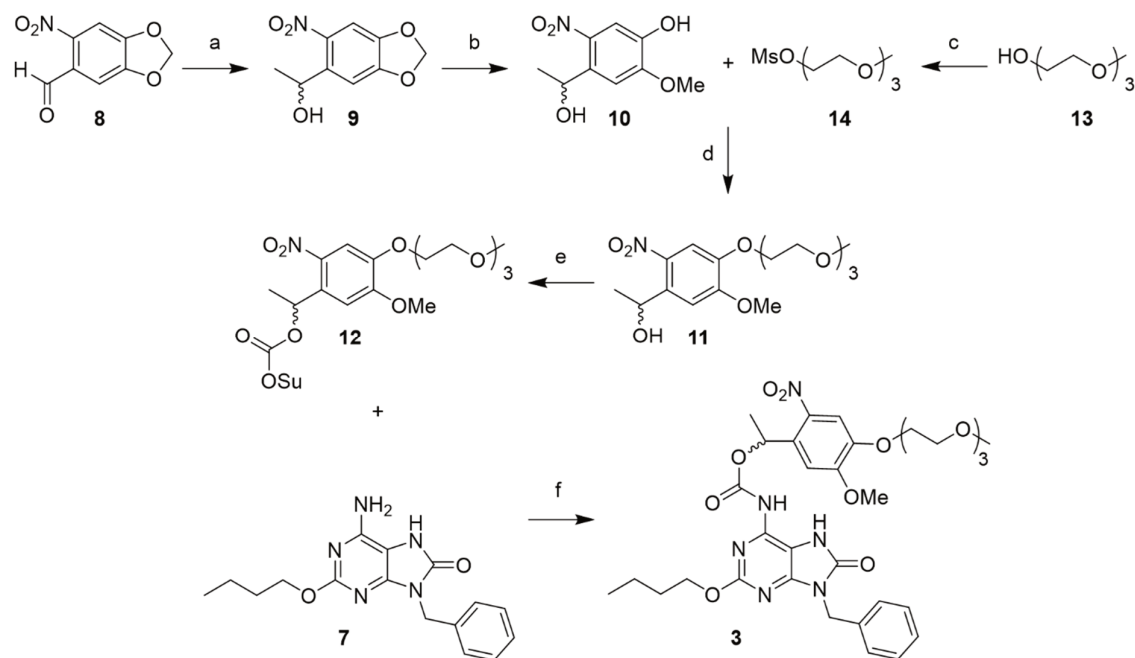
Scheme 4. a) 2M Al$_2$Me$_6$ in hexanes, DCM, r.t., qt. **b)** NaOMe, 1:2 MeOH:DMSO, 120°C, 2 hrs, 72% **c)** MsCl, TEA, DCM, 0°→RT, 1h, qt. **d)** K$_2$CO$_3$, DMF, 100°C, 2 hrs, 92% **e)** N,N'-disuccinimidyl carbonate, TEA, DMAP, DCM, r.t., o.n., 70% **f)** Compound **12**, TEA, DMAP, dioxane, 50°C, o.n., 27%.

Compound **11** was activated with N,N'-disuccinimidyl carbonate to give **12** which was used to modify to exocyclic amine of **7**, albeit in modest yields and requiring long reaction times and elevated temperatures. The resulting compound **3** was indeed soluble in aqueous media in the μM-range, and is currently awaiting biological assessment.

Two-photon labile caged TLR 2/6 ligands

It was next explored whether a 2P-sensitive photocage could be used to cage a TLR2/6 ligand. For this the NPBF was chosen as the preferred group, due to its favourable deprotection properties. First, NPBF-OH was synthesized from literature procedure without further modification.[34] Next, it was activated with N,N'-disuccinimidyl carbonate to form NPBF-OSu (**16**, Scheme **5**). **16** was then reacted with P$_2$CSTEG **17** to yield **1**, and with on-resin P2CSK$_4$ **18** to yield NPBF-P$_2$CSK$_4$ **2**. Interestingly, when a *p*-nitrophenylcarbonate activated form of NPBF was first used to attempt to cage **17**, no product formation was observed. Instead, two products formed of which one had a mass 18u lower than the starting material and the other mass 18u less than the expected product. This indicated a loss of a water molecule in both the starting material and the product during the reaction. It is suggested that the C-terminal carboxylate is able to attack the activated 4-nitrophenyl carbonate of NPBF, forming a mixed anhydride.
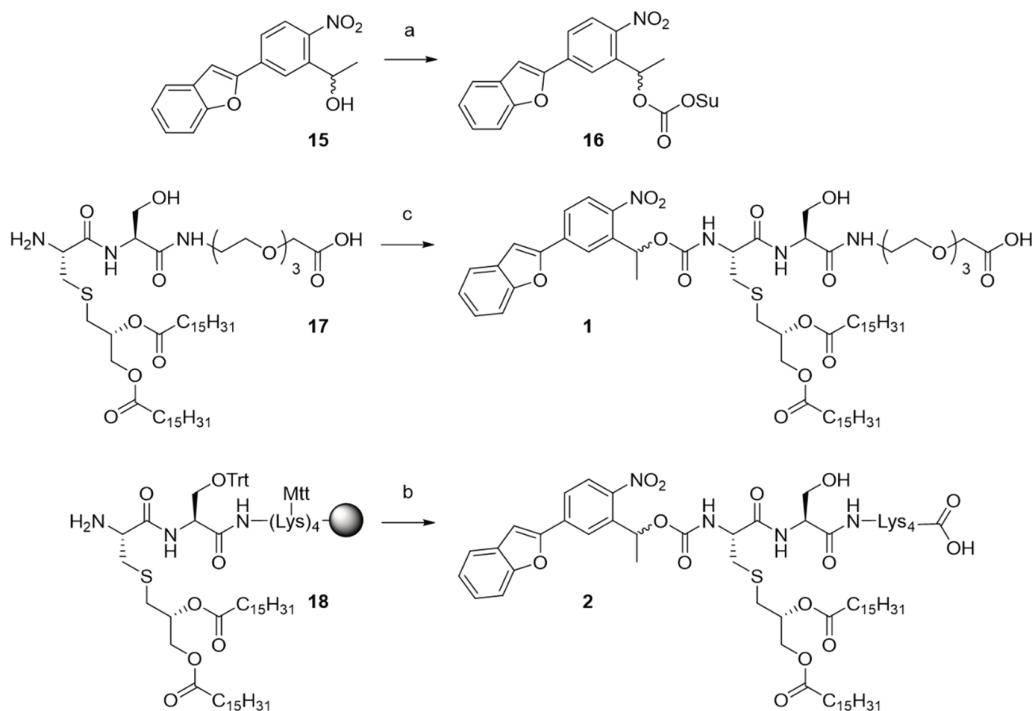
Scheme 5. a) N,N'-disuccinimidyl carbonate, TEA, DMAP, DCM, r.t., o.n., 29% **b)** i) Compound **23**, DiPEA, DMF, r.t., o.n. ii) 20% TFA in DCM, r.t., 5 min (3x), 30% overall yield **c)** Compound **16**, DiPEA, DMF, r.t., o.n., 63%.

An intramolecular cyclization with the serine alcohol or an amide then leads to a byproduct with a mass 18u lower than the parent compound. The formation of this by-product could be circumvented using the less-reactive OSu-ester of NPBF. Indeed, no byproduct formation was observed when NPBF-OSu was used to cage P$_2$CS*TEG* instead of the *p*-nitrophenylcarbonate activated NPBF to obtain compound **1**.

Compound **1** was very poorly soluble in aqueous media, and showed high adherence to plastic surfaces. Compound **2**, however, did not show these issues and therefore was used to assess the ability of NPBF to effectively shield the activity of Pam$_2$CSK$_4$ towards the TLR2/6 dimeric receptor (Figure **4**). No activity of the caged ligand towards TLR2/6-bearing THP1 cells is observed when shielded from light, except when ligand concentration is high. Only upon exposure of the treated cells with 360 nm light is NF-κB activity recovered.

Residual activity of the caged ligand at higher concentrations was also observed for the TCO-caged ligands in Chapter 2, and was addressed with the use of the C-terminally TEG-extended Pam$_2$CS ligands. Functionalization of NPBF with solubilizing moieties may enable the use of the TEG-extended ligand **1**, and was therefore investigated further, as water solubility appeared to be a continuous bottleneck for caged TLR-ligands. Compound **2** may find its use in the localized activation of human and murine TLR2/6-bearing cells.
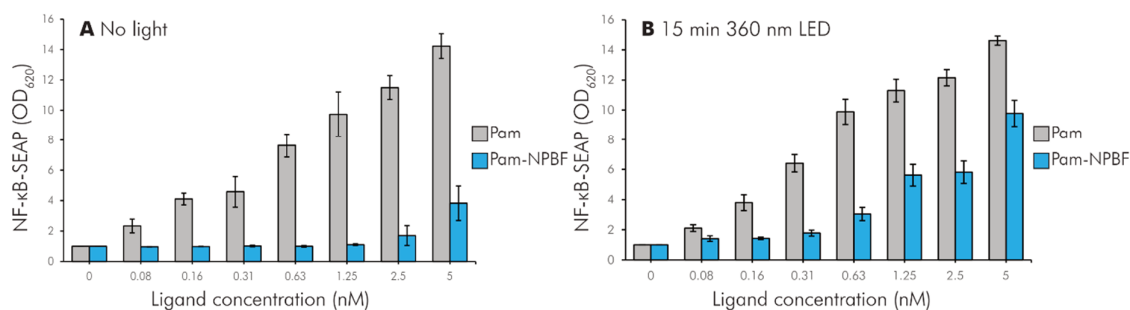
THP1 Dual

Figure 4. Activation of the NF-κB cascade in THP1 Dual cells by free ligand Pam_2CSK_4 or NPBF-caged Pam_2CSK_4 **2**, as measured through the SEAP reporter produced upon NF-κB activation. Cells were either irradiated with 360 nm light for 15 min through a 96-well plate LED array (B), or shielded from light for the same amount of time (A). At higher concentrations (>2.5 nM) caged ligand displays residual activity as reported in Chapter 2 for TCO-caged Pam_2CSK_4, but effectively shields the ligands activity towards TLR2/6 and concentrations below that. Experiment was carried out by Anya Savina (LIC).

Bis-functionalized NPBF-linker: rationalization, retrosynthetic analysis and synthesis

As the PEG-modified NVOC-TLR7 showed, the secondary functionalization of a (photo)cage can be used to allow the alteration of the biophysical properties of the molecule in a removable manner. It was postulated that the NPBF-core could serve as a platform to insert a such a secondary functionality. If – in an analogous fashion to the oNB-linkers described above – a phenol could be introduced in the backbone, it would enable the chemoselective functionalization of the phenol prior to the modification benzylic alcohol of the cage. The resulting ether functionality would also exert an electron-donating effect on the aromatic system, which is known to increase the molar attenuation coefficient thus improving absorbance at λ_{max}.[41] NPBF contains multiple potential sites for introducing a phenol group. However, literature precedence exists for the functionalization of the 5-position (Scheme **6**).[42] Additionally, having the electron-donating group (-OR) on the opposing side of the electron-withdrawing group (-NO_2) may also enhance the 2PA cross section by creating a push-pull structure through a permanent dipole moment change.[43]
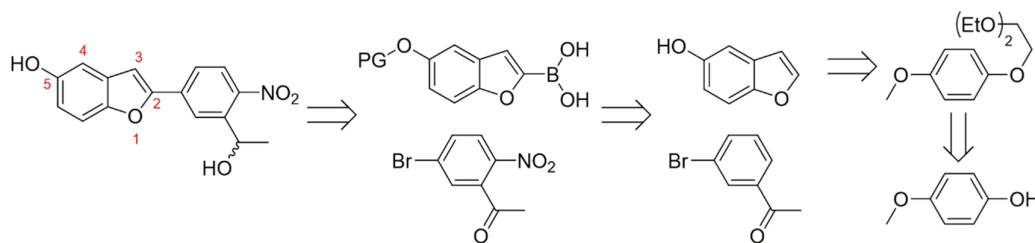
Scheme 6. Retrosynthetic analysis of NPBF diol **27**.

Scheme **6** depicts the retrosynthetic analysis of this 5-hydroxy-NPBF. The C-C bond between the benzofuran and the nitrophenyl could be formed through a Suzuki cross-coupling reaction. The nitrophenyl can be afforded by regioselective nitration of 3'-bromoacetophenone. 5-Hydroxybenzofuran can be obtained by cyclization of aryloxyacetaldehyde acetal catalyzed by

polyphosphoric acid, thus effecting 4-methoxyphenol and 3'-bromoacetophenone as the core starting materials.
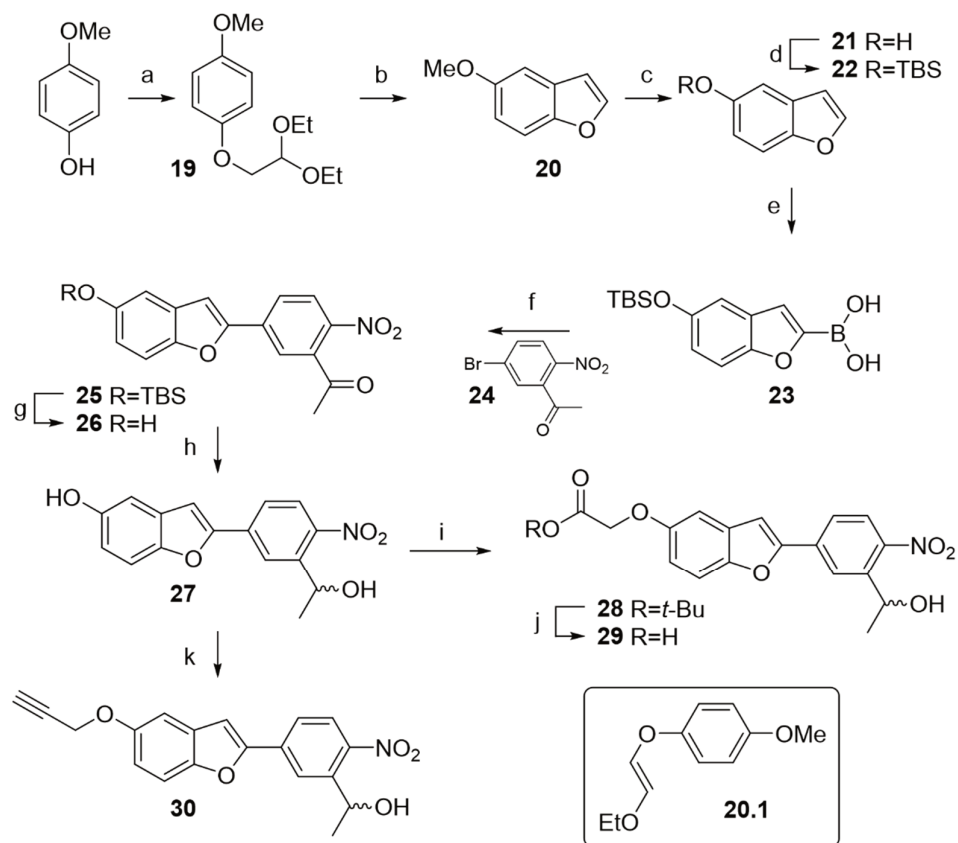
Scheme 7. a) Bromoacetaldehyde diethyl acetal, KOH, NMP, 70°C, 15 hrs, 90% **b)** Polyphosphoric acid, toluene, 110°C, 2 hrs, 33% **c)** i) BBr$_3$, DCM, -78°C → r.t., 2 hrs, 89% **d)** tert-butyldimethylsilyl chloride, imidazole, toluene, DMF, r.t., 1 hr, 70% **e)** i) n-BuLi in hexanes, THF, -78°C, 1 hr ii) triisopropyl borate, -78°C, 30 min → r.t., 30 min **f)** Pd(PPh$_3$)$_4$, K$_2$CO$_3$, 1:1 H$_2$O:THF, 66°C, 18 hrs, 61% + 14% **26** over 3 steps **g)** 70% HF in pyridine, THF, r.t., 2 hrs, 93% **h)** NaBH$_4$, MeOH, r.t., 1 hr, qt. **i)** i) tert-butyl bromoacetate, K$_2$CO$_3$, DMF, 70°C, 3 hrs, 72% **j)** TFA, DCM, r.t., 30 min, qt. **k)** i) Propargyl bromide, K$_2$CO$_3$, DMF, r.t., o.n., 98%

Scheme **7** describes the synthesis towards bis-functionalized NPBF as well as its decoration with an alkyne and carboxylic acid linker. 4-Methoxyphenol was reacted with bromoacetaldehyde diethyl acetal using potassium hydroxide as a base in NMP, a high-yielding reaction that successfully afforded **19** on a 60 g scale. The subsequent cyclization towards **20** proceeded in yields varying from 33-42%, depending on the scale of the reaction. The major byproduct was identified as a singly-eliminated ethoxide, forming the non-cyclized E-alkene **20.1**. The polyphosphoric acid reagent was somewhat unpractical to handle, but was facilitated by the use aqueous NaOH. It is interesting to note that 5-methoxybenzofuran has an extremely sweet and fruity odour and care had to be taken when handling the chemical outside the fume hood. The 5'-O-methyl proved an insufficient protecting group for the subsequent boronation and Suzuki-coupling. **20** was therefore demethylated using boron-tribromide in DCM at -78°C. This reaction did not proceed with the reported substoichiometric amounts of BBr$_3$ to full demethylation[44], so instead a molar equivalent

was used. A *tert*-butyldimethyl silyl group was installed on the 5'-OH as a protecting group after which the 2'-position was lithiated using n-BuLi. Addition of triisopropyl borate to the solution afforded compound **23**, which is used best as a crude material.

In parallel, 3'-bromoacetophenone was nitrated using a solution of cold sulfuric acid and potassium nitrate to yield **24**. When the temperature exceeds -10°C, formation of the bis-nitrated compound starts to play a significant role thus warranting close monitoring of the reaction temperature. Suzuki cross-coupling of **23** with **24** using Pd(P(Ph$_3$))$_4$ afforded a mixture of the product **25** as well as the desilylated product **26**. Purification by column chromatography to remove the palladium species before proceeding turned out to be imperative. When the crude mixture was moved forward to the desilylation reaction (using an HF.pyridine solution), an elusive palladium impurity was formed that defied removal by column chromatography or crystallization. This impurity lead to the rapid total degradation when ketone **26** was reduced with NaBH$_4$ in the following step. In the absence of this impurity the reduction proceeds smoothly and with diol **27** in hand, the 5'-OH can generally be decorated with various linkers using potassium carbonate in DMF at ambient-to-elevated temperatures (r.t. – 70°C) to obtain carboxylate **29** or propargyl **30**.

Photochemical characterization

The newly introduced phenolic alkyl-ether-substituent was postulated to have an impact on the photochemical properties of the NPBF-core. Three model compounds were synthesized to investigate this hypothesis. Boc-Lys-OMe was functionalized on the side chain amine either with NPBF-*t*-butyl ester **28**, NPBF-Alkyne **30** or NPBF **15** (Scheme 7, 8). The three derivatives were then tested to determine whether the functional groups had an effect on the photochemistry of the NPBF.
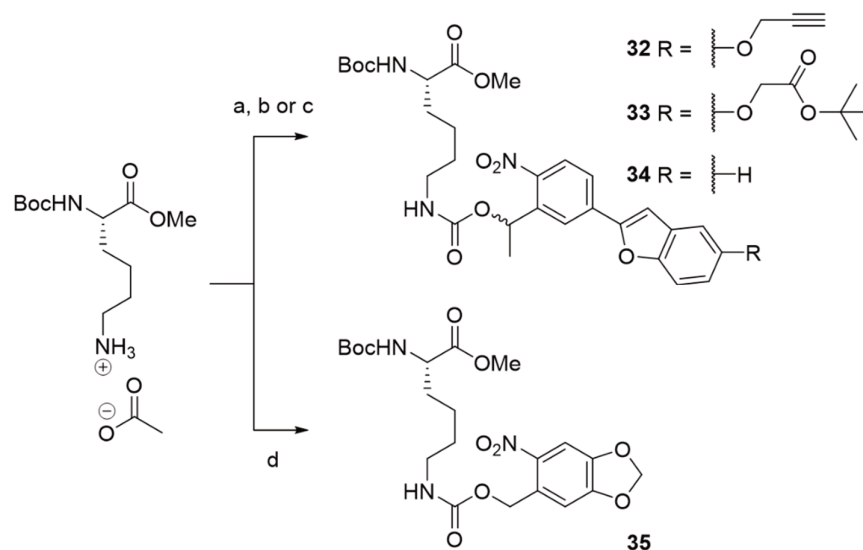
Scheme 8. Reagents and conditions: **a)** Compound **31**, DiPEA, DMF, r.t., 15 min, 66% **b)** Compound **28**, N,N'-disuccinimidyl carbonate, DiPEA, AcN, r.t., 16h, 55% **c)** Compound **16**, DiPEA, DMF, r.t., 16h, 78% **d)** Compound **36**, N,N'-disuccinimidyl carbonate, DiPEA, AcN, r.t., 1h, 75%.

First, the molar attenuation coefficient ε and λ_{max} were determined through a serial dilution in an UV-Vis spectrometer (Table **1**). The presence of the newly introduced functionality is accompanied with an increase of the ε of roughly 30%, with the λ_{max} only minimally altered. The small difference between the alkyne- and ester-modified species suggest the increase in ε is caused by the electron-donating properties of the -OR substitution, rather than any secondary effects of the functional groups.

Table 1. Molar attenuation coefficient ε measured at the λ_{max} of each model compound including standard deviation σ (n=3).

Compound	ε	σ	λ_{max}
32	16 635	88	362 nm
33	17 119	59	365 nm
34	12 945	24	357 nm
35	4248	14	349 nm

Next, the kinetics of uncaging were investigated to check whether substitution has affected this. A UV-Vis spectrum was taken at timepoint t = 0, after which the cell was irradiated with a 375 nm light source at a constant distance and power setting for 10 seconds (c ≈ 50 µM in a mixture of 1:1:1 AcN:*t*-BuOH:H$_2$O). After each irradiation interval a UV-Vis spectrum was recorded and after 1 minute of cumulative irradiation time the spectra were compounded (Figure **5**). Concentrations were normalized with respect to each compound's molar attenuation coefficient ε, such that each cuvette has the same absorption value at 360 nm at t=0. Then, the absorbance at λ = 450 nm was plotted against the irradiation time, enabling the determination of the rate with which the nitroso ketone-side product is formed and thus lysine is uncaged (Figure **6**).
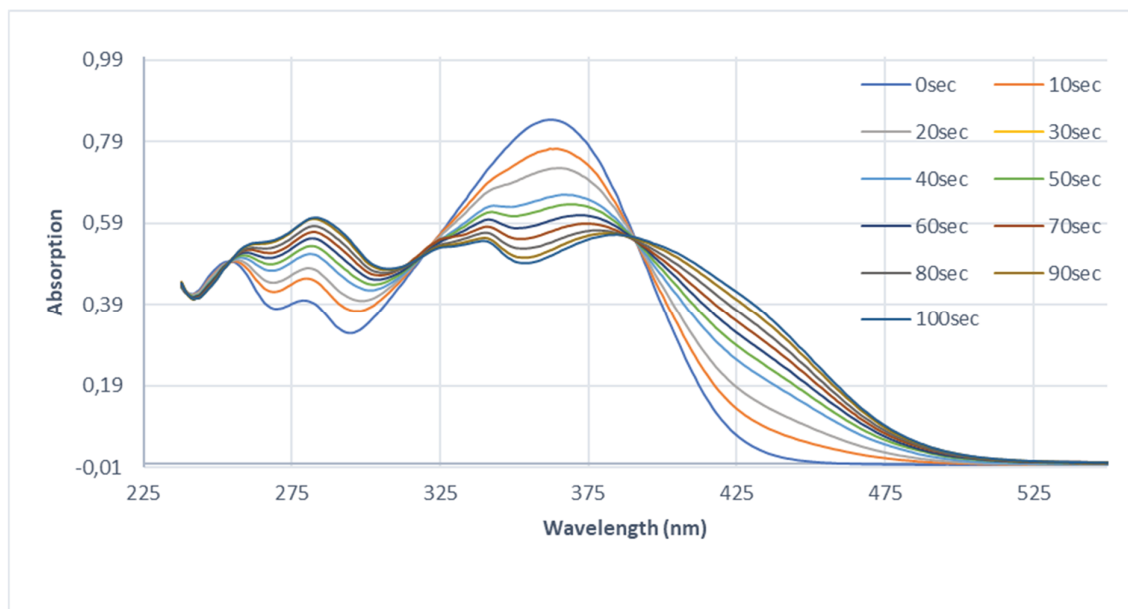

Figure 5. Example of an irradiation experiment with compound **33**. After every 10 seconds of irradiating the light source is switched off and a UV-Vis spectrum (235 – 550 nm, d=1 nm) is recorded. After a cumulative time of 100 seconds of irradiation the spectra are compounded.
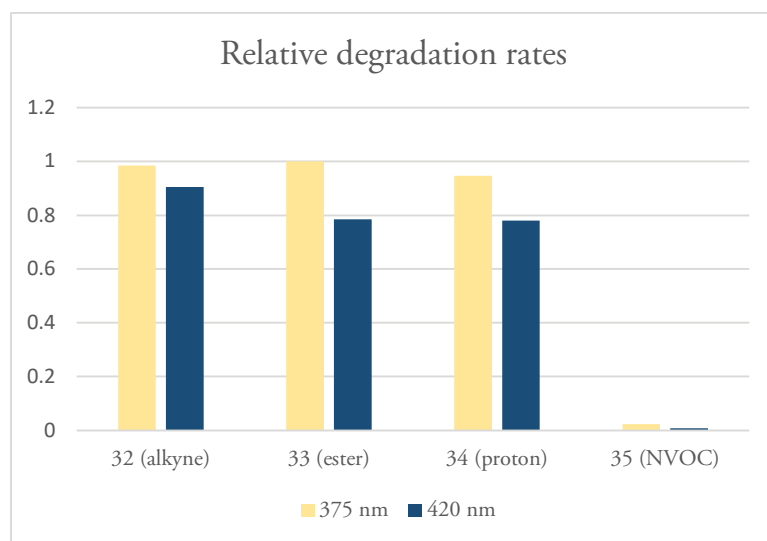
Figure 6. Relative uncaging rates at 375 nm or 420 nm irradiation.

Figure **6** depicts the relative uncaging rates for the model lysine compounds when the number of photons absorbed at the λ_{max} is the same for each sample at t = 0. There is no significant difference between the three NPBF-derivatives in regards to uncaging kinetics, meaning the newly introduced substitution does not impact the mechanism with which the photouncaging occurs in a significant manner. The rate at 420 nm appears to match the rate at 375 nm. However, these data were not corrected for the power output difference between the 375 nm LED and 420 nm LED, with the latter being approximately 4-fold brighter than the former. The NPBF-linker can thus be exploited to generate photocaged TLR ligands that are increasingly soluble in aqueous media and useable in two-photon excitation experiments.

Conclusion

In this Chapter the synthesis of various photosensitive TLR-ligands was described. In order to circumvent the poor solubility of these constructs, solubilized variants of the photoprotecting groups oNB and NPBF were developed. The 2-photon sensitive NPBF-derivatives bearing an alkyne or carboxylic acid were of particular interest due to their increase in molar extinction coefficient and the ability to use this compound as a photolinker.

Acknowledgements

Experimental section

Photochemical characterization

The irradiation experiments on the UV-Vis to characterize compounds **32-35** were performed using a custom-made experimental setup. LEDs were ordered from Roithner Lasertechnik GmbH (High Power Single Chip, H2A1 Series, 1W). Power output was measured using a radiometer on distances and settings relevant to irradiation experiments: 3 mW/cm² for 375 nm LED and 13 mW/cm² for 420 nm LED. LEDs were mounted on an aluminum heatsink that were fitted on plastic adapters (Figure **7**). These adapters were custom made for two flask sizes as well as a cuvette for UV-Vis measurements. Power output could be adapted between 50 mA-350mA in steps of 50. Spread of wavelengths emitted by the LEDs as a function of power output has been recorded by the supplier and is available online (Figure **8**).
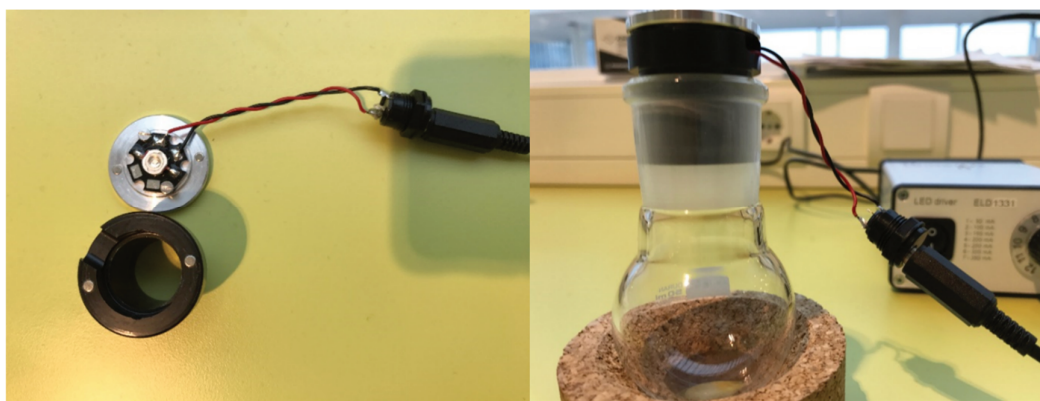

Figure 7. Custom-made photoreactor setup. A hexagonal LED is mounted on an aluminum heatsink. Magnets assist alignment and secure the LED on the black plastic adapter. Adapters have been made that fit on either flasks or a cuvette.
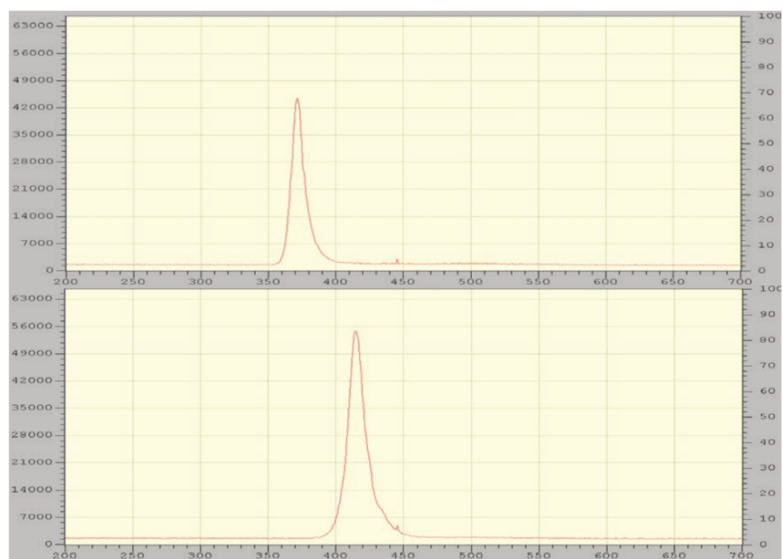

Figure 8. Normalized output power vs wavelength of the two LEDs employed in this chapter: 375 nm (top) and 420 nm (bottom). Spectra were copied from the data sheets available on the Roithner Lasertechnik website.

General methods

Commercially acquired reagents and solvents were used as received. Anhydrous solvents were prepared with activated 3 Å or 4 Å molecular sieves. All reaction progress was monitored by TLC analysis on Merck aluminum plates pre-coated with silica gel 60 and F254 fluorescent indicator; 254 nm UV light was used to check for compounds, and TLC plates were developed by charring (at approximately 150 °C) plates that were sprayed with permanganate stain (20 g/L $KMnO_4$ and 10 g/L K_2CO_3 in H_2O), unless stated otherwise. R_f values reported consider the compound being synthesized. Screening Devices silica gel (40-63 μm particle size and 60 Å pore diameter) was used during column chromatography. ^1H and ^{13}C NMR spectra were recorded on Bruker AV-400 (400 MHz) and AV-500 (500 MHz) spectrometers. Chemical shifts are reported as δ-values in ppm relative to tetramethylsilane (which was added to $CDCl_3$) or residual solvent peaks. The ^{13}C spectra are proton decoupled. LC-MS checks for all compounds were performed on a Finnigan Surveyor HPLC system with a Gemini C18 50 x 4.60 mm column, which was coupled to a Finnigan LCQ Advantage Max mass spectrometer. LC-MS samples were prepared by dissolving compounds in a tBuOH:ACN:H_2O mixture (1:1:1 by volume).
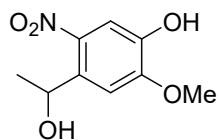
Compound 4
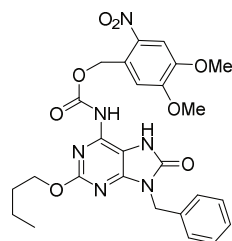
Compound **7** (50 μmol, 16 mg) was dissolved in dioxane (500 μL). DMAP (100 μmol, 12.2 mg) and NVOC-Cl (55 μmol, 16 mg) were added and the reaction was allowed to stir overnight at 50°C. LC-MS indicated over 90% conversion after which the reaction mixture was diluted with DMSO and purified by reverse phase HPLC (C18, TFA, acetonitrile/water) to afford the title compound (9.4 μmol, 5.2 mg) in a 19% yield.
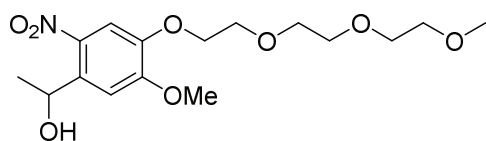
Compound 9
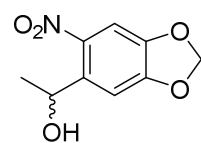
6-nitropiperonal **8** (50 mmol, 9.75 g) was dissolved in anhydrous DCM (500 mL) under a nitrogen atmosphere. Trimethylaluminum (28 mL, 2M in hexanes) was added dropwise at room temperature. After the addition was completed TLC analysis (20% EtOAc in Pnt, R_f=0.3) indicated complete conversion of the starting material. The leftover reagent was quenched by the careful addition of 1M HCl (aq.). The reaction mixture was washed with H_2O (3x), brine (1x), dried over $MgSO_4$ and concentrated *in vacuo* affording the title compound (49.8 mmol, 10.5 g) in a quantitative yield.**^{1}H NMR (400 MHz, MeOD) δ** 7.42 (s, 1H), 7.26 (s, 1H), 6.12 (dd, *J* = 4.9, 0.9 Hz, 2H), 5.34 (q, *J* = 6.3 Hz, 1H), 1.44 (d, *J* = 6.3 Hz, 3H).**^{13}C NMR (101 MHz, MeOD) δ** 148.33, 141.21, 107.13, 105.58, 104.62, 66.31, 25.21.

Compound 10

Compound **9** (49.8 mmol, 10.5 g) was dissolved in a mixture of 1:2 (v/v) anhydrous MeOH:DMSO (V_{total}=100 mL) under a nitrogen atmosphere. Sodium methoxide (150 mmol, 7.95 g) was added after which the reaction mixture was heated to 120°C. After 2 hours TLC analysis (30% EtOAc in Pnt, R_f=0.2) indicated complete conversion of the starting material. The mixture was cooled down to room temperature after which 1M HCl (aq.) was added to quench leftover reagents. The mixture was washed with EtOAc (3x). The organic layers were combined and washed with brine (1x), dried (MgSO$_4$) and concentrated *in vacuo*. The crude was adsorbed unto Celite and purified by silica gel column chromatography (20% EtOAc in Pnt → 50% EtOAc in Pnt, Δ=10%) to afford the title compound (35.8 mmol, 7.63 g) in a 72% yield. **^{1}H NMR (400 MHz, DMSO) δ** 9.92 (s, 1H), 7.41 (s, 1H), 7.31 (s, 1H), 5.41 (d, *J* = 4.3 Hz, 1H), 5.24 (dd, *J* = 6.1, 4.4 Hz, 1H), 3.89 (s, 3H), 1.35 (d, *J* = 6.2 Hz, 3H). **^{13}C NMR (101 MHz, DMSO) δ** 152.61, 145.11, 138.86, 136.53, 110.66, 109.27, 63.91, 55.96, 25.26.

Compound 11

Compound **10** (9.50 mmol, 2.02 g) was dissolved in DMF (50 mL). K$_2$CO$_3$ (10 mmol, 1.4 g) and compound **14** (10.0 mmol, 2.42 g) were added and the mixture was heated to 100 °C for 2 hours. TLC analysis (80% EtOAc in Pnt, R_f=0.2) indicated complete conversion of the starting material. The reaction mixture was poured in 1M HCl (aq.) and washed with EtOAc (3x). The organic layers were combined and washed with H$_2$O (3x), dried (MgSO$_4$), filtered and concentrated *in vacuo*. The crude was diluted with a small amount of 1:1 EtOAc:Pnt (v/v) and purified by silica gel column chromatography (50% EtOAc in Pnt) to afford the title compound (8.71 mmol, 3.13 mg) in a 92% yield. **^{1}H NMR (400 MHz, CDCl$_3$) δ** 7.63 (s, 1H), 7.30 (s, 1H), 5.55 (q, *J* = 6.3 Hz, 1H), 4.27 – 4.20 (m, 2H), 3.97 (s, 3H), 3.91 (dd, *J* = 9.4, 4.4 Hz, 2H), 3.73 (tt, *J* = 8.8, 4.2 Hz, 2H), 3.70 – 3.61 (m, 4H), 3.54 (dd, *J* = 5.7, 3.6 Hz, 2H), 3.37 (s, 3H), 1.54 (d, *J* = 6.3 Hz, 3H). **^{13}C NMR (101 MHz, CDCl$_3$) δ** 154.29, 147.03, 139.51, 137.41, 109.75, 108.82, 72.01, 71.01, 70.75, 70.66, 69.57, 69.08, 65.78, 59.14, 56.42, 24.43.
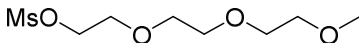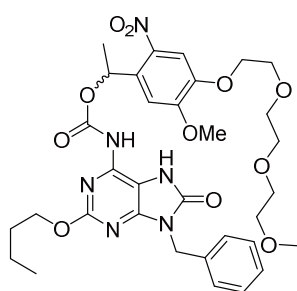
Compound 12
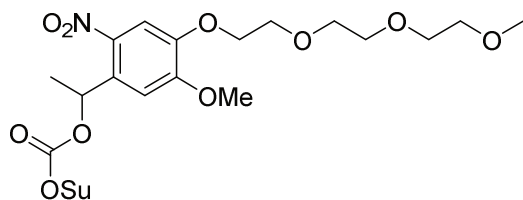
Compound **11** (0.57 mmol, 0.20 g) was dissolved in anhydrous DCM (5 mL) under a nitrogen atmosphere. Triethylamine (0.63 mmol, 87 μL) and N,N'-disuccinimidyl carbonate (1.87 mmol, 483 mg) and DMAP (0.07 mmol, 9 mg) were added and the mixture was allowed to stir at room temperature overnight. TLC analysis (80% EtOAc in Pnt, triethylamine-neutralized, R_f=0.4, purple under 365 nm UV) indicated complete conversion of the starting material. The crude was adsorbed onto Celite and purified by silica gel column chromatography (triethylamine-neutralized, 60% EtOAc in Pnt → 80% EtOAc in Pnt) to afford the title compound (0.40 mmol, 0.20 g) in a 70% yield. **^{1}H NMR (400 MHz, CDCl$_3$) δ**

7.72 (s, 1H), 7.07 (s, 1H), 6.49 (q, *J* = 6.3 Hz, 1H), 4.25 (dd, *J* = 10.9, 6.0 Hz, 2H), 4.04 (s, 3H), 3.95 – 3.88 (m, 2H), 3.77 – 3.71 (m, 2H), 3.66 (ddd, *J* = 15.6, 7.1, 4.4 Hz, 4H), 3.55 (dd, *J* = 5.6, 3.6 Hz, 2H), 3.37 (s, 3H), 2.80 (s, 4H), 1.76 (d, *J* = 6.4 Hz, 3H). **¹³C NMR (101 MHz, CDCl₃) δ** 168.61, 154.64, 150.56, 147.73, 139.09, 131.31, 109.65, 107.35, 76.52, 71.87, 70.88, 70.60, 70.52, 69.37, 68.99, 58.99, 56.49, 25.39, 21.88.
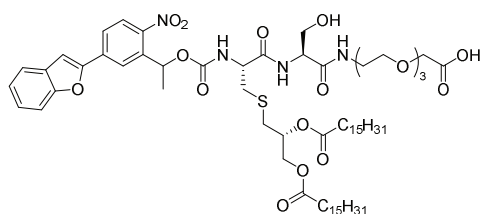
Compound 14

Triethylene glycol monomethyl ether **13** (10.0 mmol, 1.61 mL) was dissolved in anhydrous DCM (10 mL). Triethylamine (20.0 mmol, 2.77 mL) was added and the mixture was cooled to 0°C. Mesyl chloride (12.0 mmol, 932 µL) was added carefully after which the mixture was allowed to stir for 1 hour at room temperature. TLC analysis 850% EtOAc in Pnt, R_f=0.3) indicated complete conversion of the starting material. The mixture was diluted with DCM and washed with 1M HCl (aq.) (3x) and consequently a saturated solution of NaHCO₃ (aq.) (3x). The organic layer was dried (MgSO₄), filtered and concentrated *in vacuo* to afford the title compound (10.0 mmol, 2.42 g) in a quantitative yield. **¹H NMR (400 MHz, CDCl₃) δ** 4.41 – 4.33 (m, 1H), 3.80 – 3.73 (m, 1H), 3.72 – 3.59 (m, 3H), 3.56 – 3.49 (m, 1H), 3.37 (s, 1H), 3.08 (s, 1H). **¹³C NMR (101 MHz, CDCl₃) δ** 71.87, 70.59, 70.51, 69.36, 68.99, 59.01, 37.68.

Compound 3

Compound **7** (50 µmol, 16 mg) was dissolved in dioxane (100 µL). Triethylamine (150 µmol, 21µL), DMAP (8 µmol, 1 mg) and compound **12** (55 µmol, 29 mg) were added and the reaction was allowed to shake overnight at 50°C. LC-MS indicated over 90% conversion after which the reaction mixture was diluted with DMSO and purified by reverse phase HPLC (C18, TFA, acetonitrile/water) to afford the title compound (13.5 µmol, 9.4 mg) in a 27% yield.
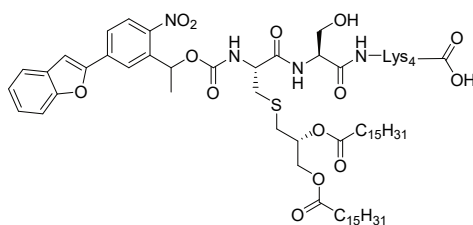
Compound 1

Compound **17** (2.4 µmol, 2.3 mg, synthesis described in Chapter 2) was dissolved in DMF (500 µL). DiPEA (10 µmol, 1.8 µL) and compound **16** (5.9 µmol, 2.5 mg) were added and the reaction was allowed to shake overnight at room temperature. LC-MS analysis indicated complete conversion of the starting material. The mixture was concentrated *in vacuo* and co-evaporated with toluene (3x). The crude was dissolved in DCM and purified by silica gel column chromatography (DCM →1% MeOH in DCM →10% MeOH in DCM) to afford the *tert*-butyl protected intermediate product. The product was dissolved in DCM (1 mL) and TFA was added (1 mL) and the reaction was stirred for 2 hours at room temperature. TLC analysis (5% MeOH in DCM, R_f=0.3) indicated complete conversion of the reaction and the mixture was concentrated *in vacuo* to afford the title compound (1.5 µmol, 1.9 mg) in a 63% yield.
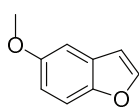
Compound 2

Resin-bound hexapeptide (10 µmol, 45 mg, synthesis described in Chapter 2) was swollen in DMF. DiPEA (11 µmol, 2.0 µL) and compound **16** (50 µmol, 21 mg) were added and the reaction was allowed to shake overnight at room temperature. A small amount of TFA-treated resin analyzed by LC-MS indicated complete conversion of the starting material. The resin was washed with DMF (3x) and treated with a solution of 20% TFA in DCM. The solution was dropped in a mixture of 1:1 Et$_2$O:Pnt (v/v) at -30°C. The product was allowed to precipitate overnight at -30°C after which the precipitate was collected by centrifugation. The precipitate was dissolved in DMSO and purified by reverse-phase HPLC (C18, TFA, acetonitrile/water) to afford the title compound (3.0 µmol, 4.7 mg) in a 30% overall yield.
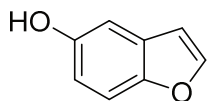
Compound 19
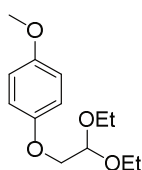
A procedure from literature [1] was modified as follows: 4-methoxyphenol (300 mmol, 37.2 g) was dissolved in NMP (300 mL, 1 M) followed by addition of potassium hydroxide (600 mmol, 33.6 g) at r.t.. Bromoacetaldehyde diethyl acetal (7.5 mmol, 1.13 mL) was added slowly and the reaction was stirred at 70°C for 15 h. TLC analysis indicated complete conversion of the starting material (10% Et$_2$O in Pnt, R$_f$=0.7). The reaction mixture was poured in H$_2$O and extracted with Et$_2$O (3x). The combined organic layers were washed with brine (1x), dried over MgSO$_4$ and concentrated *in vacuo*. Purification by silica gel column chromatography (5% Et$_2$O → 10% Et$_2$O in Pnt) yielded compound **19** (270 mmol, 64.9 g, 90%). **¹H NMR (400 MHz, Chloroform-*d*) δ** 6.90 – 6.76 (m, 4H), 4.80 (t, *J*=5.2, 1H), 3.95 (d, *J*=5.2, 2H), 3.80 – 3.68 (m, 2H), 3.72 (s, 3H), 3.61 (dq, *J*=9.4, 7.0, 2H), 1.23 (t, *J*=7.1, 6H). **¹³C NMR (101 MHz, CDCl₃) δ** 153.94, 152.71, 115.53, 114.46, 100.49, 69.13, 62.36, 55.48, 15.26.
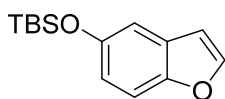
Compound 20

A procedure from literature[2] was modified as follows: Polyphosphoric acid (60 g, H$_3$PO$_4$ basis, 115%) was dissolved in toluene (600 mL) and the mixture was heated to 110°C under vigorous stirring. Compound **19** (255 mmol, 61.3 g) was dissolved in toluene (160 mL, 1.6 M) and was dropwise added to the solution over the course of 1 hour. After stirring for 1 hour at reflux temperature TLC indicated complete conversion of the starting material (5% Et$_2$O in Pnt, R$_f$=0.8). The mixture was cooled to r.t., decanted in 1 M NaOH (aq) and extracted with toluene. The combined organic layers were washed with brine (1x), dried over MgSO$_4$ and concentrated *in vacuo*. Purification by silica gel column chromatography (Pnt → 2% Et$_2$O in Pnt) yielded compound **20** (83.1 mmol, 12.3 g, 33%). **¹H NMR (400 MHz, Chloroform-*d*) δ** = 7.59 (dd, *J*=2.2, 0.5, 1H), 7.39 (ddd, *J*=8.9, 1.0, 0.5, 1H), 7.05 (d, *J*=2.6, 1H), 6.90 (ddd, *J*=8.9, 2.6, 0.5, 1H), 6.70 (dd, *J*=2.2, 0.9, 1H), 3.84 (s, 3H). **¹³C NMR (101 MHz, CDCl₃) δ** = 145.86, 128.08, 113.20, 111.93, 106.82, 103.61, 56.03.
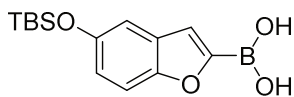
Compound 21

A procedure from literature[3] was modified as follows: Compound **20** (5.7 mmol, 849 mg) was dissolved in anhydrous DCM (8.1 mL, 0.7 M) under a nitrogen atmosphere. The mixture was cooled to -78°C after which a 1 M solution of BBr$_3$ in DCM (6.8 mmol, 6.8 mL) was slowly added. The mixture was stirred at -78°C for 1 hour and then heated to r.t. and stirred for an additional hour. TLC analysis indicated complete conversion of the starting material (20% EtOAc in Pnt, R$_f$=0.7). The reaction was quenched with saturated solution of NaHCO$_3$ (aq.), poured in H$_2$O and extracted with EtOAc (3x). The combined organic layers were washed with brine (1x), dried over MgSO$_4$ and concentrated *in vacuo*. Purification with silica gel column chromatography (5% EtOAc → 10% EtOAc in Pnt) yielded compound **21** (5.11 mmol, 0.685 g, 89**%**). **¹H NMR (400 MHz, Chloroform-*d*) δ** = 7.59 (dd, *J*=2.2, 0.5, 1H), 7.35 (ddd, *J*=8.8, 1.0, 0.5, 1H), 7.01 (dd, *J*=2.6, 0.6, 1H), 6.81 (ddd, *J*=8.8, 2.6, 0.5, 1H), 6.67 (dd, *J*=2.2, 0.9, 1H), 4.89 (s, 1H). **¹³C NMR (101 MHz, CDCl$_3$) δ** = 146.12, 113.05, 111.92, 106.56, 106.21.

Compound 22

Compound **21** (3.73 mmol, 0.501 g) was dissolved in anhydrous DMF (3.8 mL, 1 M) under a nitrogen atmosphere. A 50 wt% solution of *tert*-butyldimethylsilyl chloride in toluene (11.3 mmol, 3.9 mL, 2.9 M) was added followed by the addition of imidazole (18.7 mmol, 1.27 g). The mixture was stirred for 1 hour at r.t.. TLC analysis indicated complete conversion of the starting material (1% Et$_2$O in Pnt, R$_f$= 0.7). The mixture was then poured in H$_2$O and extracted with Et$_2$O (3x). The combined organic layers were washed with brine (1x), dried over MgSO$_4$ and concentrate *in vacuo*. Purification with silica gel column chromatography (Pnt → 1% Et$_2$O in Pnt) yielded compound **22** (2.62 mmol, 0.65 g, 70.2%). **¹H NMR (400 MHz, Chloroform-*d*) δ** = 7.60 (d, *J*=2.1, 1H), 7.38 (dd, *J*=8.8, 0.9, 1H), 7.06 (d, *J*=2.5, 1H), 6.85 (dd, *J*=8.8, 2.4, 1H), 6.69 (dd, *J*=2.2, 0.9, 1H), 1.05 (d, *J*=0.9, 10H), 0.24 (d, *J*=0.8, 6H). **¹³C NMR (101 MHz, CDCl$_3$) δ** = 151.50, 150.46, 145.75, 128.22, 117.63, 111.61, 111.10, 106.69, 30.45, 25.88, 18.35, -4.33.
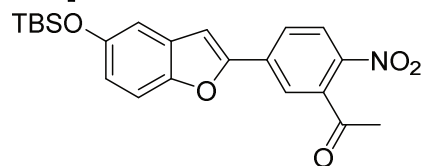
Compound 23

Compound **22** (3.65 mmol, 0.906 g) was dissolved in anhydrous THF (20 mL, 0.2 M) under a nitrogen atmosphere and cooled to -78°C. A 1.6 M solution of n-butyllithium in hexanes (8.0 mmol, 5.02 mL) was added dropwise and the mixture was stirred for 1 hour. Triisopropyl borate (4.4 mmol, 1.0 mL) was added dropwise and the mixture was stirred for another 30 min. The mixture was then heated to r.t. and stirred for an additional 30 min. The reaction mixture was quenched with a 2 M solution of HCl (aq.) (4 mL, 8 mmol), poured in H$_2$O and extracted with EtOAc (3x). The combined organic layers were washed with H$_2$O (1x) and brine (1x), dried over MgSO$_4$ and concentrated *in vacuo*. The crude product **23** was used as is in the following reaction.
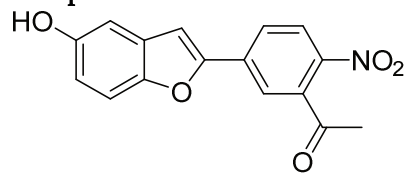
Compound 24
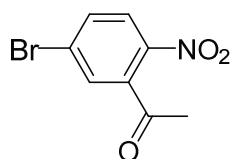
KNO$_3$ (24.0 mmol, 2.42 g) was loaded into a flask and cooled down to -20°C. H$_2$SO$_4$ (21.75 mL, 98%) was added and the mixture was stirred for 30 min. 3'-bromoacetophenone (20 mmol, 3.98 g, 2.64 mL) was slowly added. The reaction mixture was heated up to -10°C and stirred for another 2 h. The reaction mixture was poured into crushed ice and extracted with DCM (3x). The combined organic layers were washed with brine (1x), dried over MgSO$_4$ and concentrated *in vacuo*. The crude was dissolved in a minimal amount of Et$_2$O after which Pnt was added until a precipitation was visible. The suspension was gently warmed until the precipitate dissolved again. The product was allowed to crystallize out of solution until no more formation of crystals was observed. The crystals were collected and washed with cold Pnt yielding compound **24** (9.8 mmol, 2.4 g, 49%). **^{1}H NMR (400 MHz, Chloroform-*d*) δ** = 8.00 (d, *J*=8.7, 1H), 7.74 (dd, *J*=8.7, 2.1, 1H), 7.55 (d, *J*=2.1, 1H), 2.56 (s, 3H). **^{13}C NMR (101 MHz, CDCl$_3$) δ** = 133.75, 130.47, 126.05, 30.37.
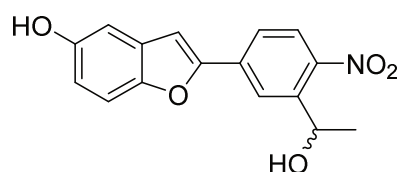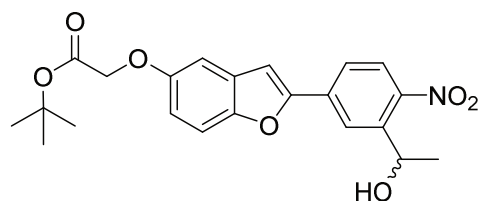
Compound 25

Compound **23** (4.62 mmol, 1.35 g) and compound **24** (3.65 mmol, 0.89 g) were dissolved in a 1:1 mixture of THF and H$_2$O (42 mL) under a nitrogen atmosphere. The flask was wrapped in aluminum foil and K$_2$CO$_3$ (5.48 mmol, 0.757 g) and Pd(Ph$_3$)$_4$ (0.23 mmol, 0.266 g) were added. The mixture was heated to 66°C and refluxed for 18 h. TLC analysis indicated complete conversion of the starting material (10% Et$_2$O in Pnt, R$_f$=0.3). The reaction mixture was quenched using a saturated solution of NH$_4$Cl (aq.), poured in H$_2$O and extracted with EtOAc (3x). The combined organic layers were washed with brine (1x), dried over MgSO$_4$ and concentrated *in vacuo*. The crude mixture consists of partially desilylated product, so the crude mixture can be used as is in the following reaction. Purification with silica gel column chromatography (5% Et$_2$O → 30% Et$_2$O in Pnt) yielded compound **25** (2.23 mmol, 0.919 g, 61%). Increasing the polarity of the eluent (30% Et$_2$O in Pnt → 30% EtOAc in Pnt) yielded prematurely desilylated compound **26** (0.51 mmol, 0.15 g, 14%).**^{1}H NMR (400 MHz, Chloroform-*d*) δ** = 8.09 (d, *J*=8.6, 1H), 7.87 (dd, *J*=8.6, 1.9, 1H), 7.76 (d, *J*=1.8, 1H), 7.36 (dt, *J*=8.9, 0.8, 1H), 7.13 (d, *J*=0.9, 1H), 7.05 (d, *J*=2.4, 1H), 6.89 (dd, *J*=8.8, 2.5, 1H), 2.61 (s, 3H), 1.04 (d, *J*=0.7, 13H), 0.25 (d, *J*=0.7, 7H). **^{13}C NMR (101 MHz, CDCl$_3$) δ** = 199.76, 152.82, 152.03, 150.87, 144.03, 139.06, 136.13, 129.17, 125.65, 125.14, 122.72, 119.69, 111.72, 111.24, 105.94, 30.24, 25.69, 18.18, -4.48.

Compound 26

Compound **25** (0.66 mmol, 0.27 g) was dissolved in anhydrous THF (7 mL) under a nitrogen atmosphere. A solution of 70% HF in Pyridine (0.7 mL, 10 vol%) was added and the reaction was stirred at r.t. for 2 h. TLC analysis indicated complete conversion of the starting material (30% EtOAc in Pnt, R_f=0.2). The reaction was quenched with a saturated solution of $NaHCO_3$ (aq.) until no CO_2 release was observed. The mixture was poured into H_2O and extracted with EtOAc (3x). The combined organic layers were washed with brine (1x), dried over $MgSO_4$ and concentrated *in vacuo*. Purification with silica gel column chromatography (15% EtOAc → 30% EtOAc in Pnt) yielded compound **26** (0.62 mmol, 0.18 g, 93%). **¹H NMR (400 MHz, DMSO-d_6) δ** = 9.40 (s, 1H), 8.22 (d, *J*=8.4, 1H), 8.17 – 8.09 (m, 2H), 7.67 (s, 1H), 7.47 (d, *J*=8.8, 1H), 7.01 (d, *J*=2.5, 1H), 6.86 (dd, *J*=8.9, 2.5, 1H), 2.63 (s, 3H). **¹³C NMR (101 MHz, DMSO) δ** = 199.78, 153.96, 152.61, 149.26, 144.26, 138.03, 135.30, 129.18, 126.15, 125.61, 123.21, 115.36, 111.85, 106.77, 105.83, 30.06.
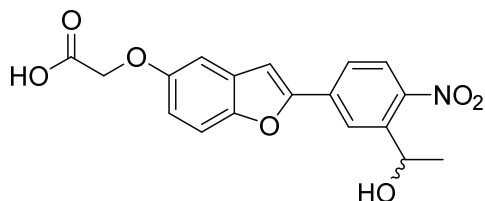
Compound 27

Compound **26** (0.36 mmol, 0.106 g) was dissolved in methanol (3.6 mL, 0.1 M) and the mixture was cooled down to 0°C. $NaBH_4$ (0.54 mmol, 0.020 g) was added in portions. After addition the mixture was heated to r.t. and stirred for 1 hour. TLC analysis indicated full conversion of the starting material (30% EtOAc in Pnt, R_f=0.2). The mixture was concentrated *in vacuo* after which it was poured in H_2O and extracted with EtOAc (3x). The combined organic layers were washed with brine (1x) and dried over $MgSO_4$. Concentration *in vacuo* yielded compound **27** (0.36 mmol, 108 mg, 100%). **¹H NMR (400 MHz, DMSO-d_6) δ** = 9.36 (s, 1H), 8.29 (d, *J*=1.9, 1H), 8.04 (d, *J*=8.5, 1H), 7.96 (dd, *J*=8.5, 1.9, 1H), 7.57 (d, *J*=0.9, 1H), 7.49 (d, *J*=8.9, 1H), 7.00 (d, *J*=2.4, 1H), 6.83 (dd, *J*=8.8, 2.5, 1H), 5.66 (d, *J*=4.3, 1H), 5.30 – 5.20 (m, 1H), 1.43 (d, *J*=6.3, 3H). **¹³C NMR (101 MHz, DMSO) δ** = 153.85, 146.24, 143.61, 143.61, 134.44, 129.31, 125.17, 123.70, 123.04, 114.82, 111.77, 105.74, 105.50, 64.01, 25.09.

Compound 28

Compound **27** (0,154 g; 0,51 mmol) was dissolved in dry DMF (1,7 mL) in nitrogen atmosphere. K_2CO_3 (0.62 mmol, 0.083 g) and *t*-butyl bromoacetate (0.95 mmol, 0.14 mL) were added and the reaction was stirred at 70°C for 3 h. TLC analysis indicated complete conversion of the starting material (30% EtOAc in Pnt, R_f=0.8). The reaction mixture was poured into H_2O and extracted with EtOAc (3x). The combined organic layers were washed with H_2O (1x) and brine (1x), dried over $MgSO_4$ and concentrated *in vacuo*. Purification with silica gel column chromatography (20% EtOAc in Pnt) yielded compound **28** (0.36 mmol, 0.149 g, 72%). **¹H NMR (300 MHz, Chloroform-d) δ** = 8.25 (d, *J*=2.0, 1H), 7.96 (d, *J*=8.6, 1H), 7.72 (dd, *J*=8.6, 1.9, 1H), 7.43 – 7.33 (m, 1H), 7.06 (d, *J*=0.9, 1H), 7.00 –

6.89 (m, 2H), 5.52 (q, *J*=6.3, 1H), 4.51 (s, 2H), 3.02 (s, 1H), 1.60 (d, *J*=6.3, 3H), 1.50 (s, 9H).^{13}**C NMR (75 MHz, CDCl₃) δ** = 168.35, 154.62, 154.30, 150.83, 146.41, 142.82, 135.33, 129.24, 125.38, 123.69, 123.61, 115.11, 112.10, 105.10, 104.91, 82.62, 66.63, 65.70, 53.56, 28.11, 24.57.
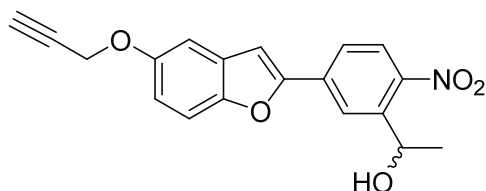
Compound 29

Compound **28** (0.21 mmol, 0.086 g) was dissolved in DCM (2 mL). Trifluoroacetic acid (2 mL) was added and the reaction was stirred at r.t. for 30 min. TLC analysis indicated complete conversion of the starting material (30% EtOAc in Pnt, R$_f$=0.1). The mixture was concentrated *in vacuo*. Co-evaporation with DCM (3x), toluene (3x) and CHCl₃ (1x) yielded compound **29** (0.21 mmol, 0.075 g, quant.). **¹H-NMR (400 MHz, DMSO-*d₆*) δ** = 13.03 (s, 1H), 8.32 (d, *J* = 1.7 Hz, 1H), 8.05 (d, *J* = 8.6 Hz, 1H), 8.00 (dd, *J* = 8.6, 1.8 Hz, 1H), 7.65 (s, 1H), 7.62 (d, *J* = 9.1 Hz, 1H), 7.19 (d, *J* = 2.6 Hz, 1H), 7.01 (dd, *J* = 8.9, 2.6 Hz, 1H), 5.66 (s, 1H), 5.25 (q, *J* = 6.3 Hz, 1H), 4.73 (s, 2H), 1.44 (d, *J* = 6.3 Hz, 3H).**¹³C-NMR (100 MHz, DMSO-*d₆*): δ** 170.36, 154.52, 153.93, 149.96, 143.60, 134.22, 129.11, 125.17, 123.88, 123.17, 115.02, 112.09, 105.68, 104.86, 65.19, 64.02, 25.09.
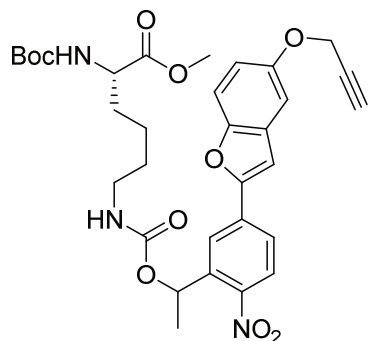
Compound 30

Compound **27** (0.50 mmol, 0.15 g) was dissolved in DMF (0.2 M, 2.5 mL). K₂CO₃ (1.92 mmol, 0.265 g) was added and the reaction mixture was stirred for 1 hour at r.t.. Propargyl bromide (1.2 mmol, 108 μL) was added to the reaction and the mixture was stirred overnight. TLC analysis indicated full conversion the starting material (30% EtOAc in Pnt, R$_f$=0.7). The reaction was quenched with a saturated solution of NH₄Cl (aq.) and extracted with EtOAc (3x). The combined organic layers were washed with brine (1x) and concentrated *in vacuo*. Purification with silica gel column chromatography (10% EtOAc → 15% EtOAc in Pnt) yielded compound **30** (0.49 mmol, 0.16 g, 98%). **¹H NMR (400 MHz, Acetone-*d₆*) δ** = 8.40 (d, *J*=2.0, 1H), 7.97 (d, *J*=8.6, 1H), 7.89 (dd, *J*=8.5, 2.0, 1H), 7.50 (d, *J*=9.0, 1H), 7.43 (d, *J*=0.9, 1H), 7.24 (d, *J*=2.6, 1H), 7.01 (dd, *J*=9.0, 2.6, 1H), 5.44 (qd, *J*=6.3, 4.3, 1H), 4.78 (dd, *J*=5.4, 3.3, 3H), 3.07 (t, *J*=2.4, 1H), 1.51 (d, *J*=6.3, 3H). **¹³C NMR (101 MHz, Acetone-*d₆*) δ** = 155.31, 151.46, 147.54, 144.47, 135.62, 130.29, 129.66, 125.82, 124.45, 124.30, 116.12, 112.69, 112.20, 106.20, 105.94, 79.84, 77.00, 65.57, 65.47, 57.00, 25.45, 25.39.
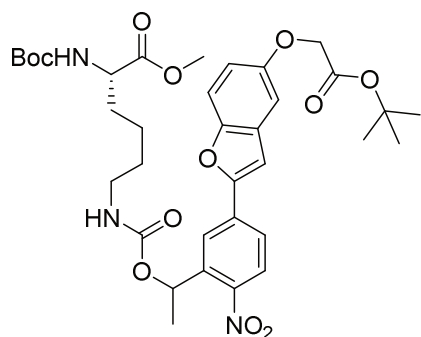
Compound 31
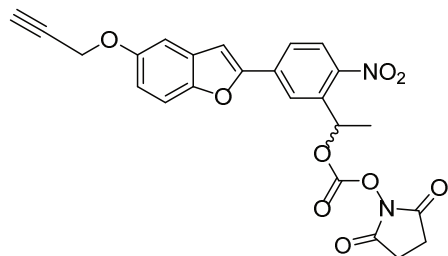
Compound **30** (0.42 mmol, 0.151 g) was dissolved in anhydrous DMF (2.2 mL, 0.2 M) under a nitrogen atmosphere. Disuccinimidyl carbonate (0.63 mmol, 0.16 g) and triethylamine (1.3 mmol, 0.18 mL) were added and the reaction mixture was stirred at r.t. overnight. TLC analysis indicated complete conversion of the starting material (30% EtOAc in Pnt, R_f=0.4). The mixture was concentrated *in vacuo* and diluted with H_2O. The aqueous layer was extracted with DCM (3x) after which the combined organic layers were washed with brine (1x), dried over $MgSO_4$ and concentrated *in vacuo*. The crude product was adsorbed on Celite. Purification with silica gel column chromatography (DCM → 0.25% MeOH in DCM) yielded compound **31** (0.30 mmol, 143 mg, 71%). **¹H-NMR (400 MHz, DMSO-d_6):** **δ** = 8.21 (d, *J* = 1.7, 1H), 8.19 (d, *J* = 8.7, 1H), 8.14 (dd, *J* = 8.6, 1.8, 1H), 7.80 (s, 1H), 7.65 (d, *J* = 9.0, 1H), 7.32 (d, *J* = 2.6, 1H), 7.06 (dd, *J* = 9.0, 2.6, 1H), 6.34 (q, *J* = 6.4, 1H), 4.86 (d, *J* = 2.3, 2H), 3.59 (t, *J* = 2.3, 1H), 2.79 (d, *J* = 14.0, 4H), 1.81 (d, *J* = 6.5, 2H).
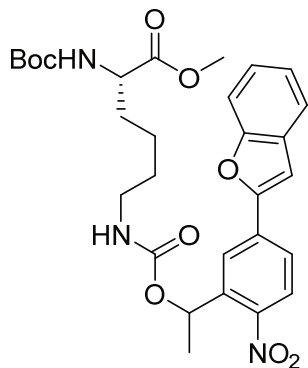
Compound 32

Compound **31** (0.09 mmol, 0.056 g) was dissolved in DMF (1 mL). Boc-Lys-OMe.HOAc (0.5 mmol, 0.130 g) and DiPEA (1 mmol, 174 μL) was added. The reaction mixture was stirred for 15 min at r.t.. TLC analysis indicated complete conversion of the starting material (5% MeOH in DCM, R_f=0.6). The reaction mixture was poured in a 50% brine solution which was washed with EtOAc (3x). The combined organic layers were washed with 0.1M HCl (aq.) (2x), brine (3x), dried ($MgSO_4$) and concentrated *in vacuo*. Purification with silica gel column chromatography (DCM → 0.5% MeOH in DCM) yielded compound **32** (0.059 mmol, 0.037 g, 66%). **¹H NMR (400 MHz, Chloroform-*d*) δ** = 8.08 − 8.00 (m, 2H), 7.82 (dt, *J*=8.5, 1.8, 1H), 7.47 (d, *J*=8.9, 1H), 7.18 (t, *J*=3.3, 2H), 7.03 (ddd, *J*=9.0, 2.6, 1.0, 1H), 6.33 (qd, *J*=6.4, 3.4, 1H), 5.06 (d, *J*=8.4, 1H), 5.00 (d, *J*=6.9, 1H), 4.75 (d, *J*=2.4, 2H), 4.27 (d, *J*=7.0, 1H), 3.70 (d, *J*=5.1, 3H), 3.13 (ddd, *J*=35.2, 13.1, 6.8, 1H), 3.13 (s, 1H), 2.56 (t, *J*=2.4, 1H), 1.74 (s, 1H), 1.68 (dd, *J*=6.5, 1.8, 3H), 1.44 (d, *J*=5.0, 11H), 1.36 (td, *J*=10.1, 9.0, 4.0, 2H), 1.26 (s, 1H).**¹³C NMR (101 MHz, CDCl₃) δ** = 155.43, 154.35, 150.98, 146.66, 140.18, 135.39, 129.30, 125.56, 124.17, 123.09, 115.56, 112.16, 105.53, 105.05, 78.74, 75.75, 56.79, 53.15, 52.42, 40.77, 32.60, 28.43, 22.52, 22.37.
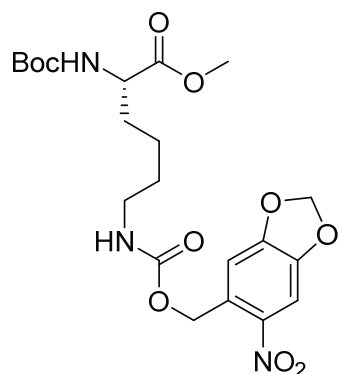
Compound 33

Compound **28** (0.17 mmol, 0.070 g) was dissolved in acetonitrile (1 mL). N,N'-disuccinimidyl carbonate (0.50 mmol, 0.13 g) and DiPEA (0.30 mmol, 52 μL) were added and the mixture was stirred for 16 h at r.t.. The reaction mixture was poured in a 50% brine solution which was washed with EtOAc (3x). The combined organic layers were washed with brine (1x), dried (MgSO$_4$) and concentrated *in vacuo*. The concentrate was reconstituted in DMF (2 mL) and boc-Lys-OMe.HOAc (0.50 mmol, 0.13 g) and DiPEA (1.0 mmol, 174 μL) was added. The reaction mixture was stirred for 15 min at r.t.. TLC analysis indicated complete conversion of the starting material (5% MeOH in DCM, R$_f$=0.6). The reaction mixture was poured in a 50% brine solution which was washed with EtOAc (3x). The combined organic layers were washed with 0.1M HCl (aq.) (2x), brine (3x), dried (MgSO$_4$) and concentrated *in vacuo*. Purification with silica gel column chromatography (DCM → 0.5% MeOH in DCM) yielded compound **33** (0.093 mmol, 0.065 g, 55%). **¹H NMR (400 MHz, Chloroform-*d*) δ** = 8.08 – 7.99 (m, 2H), 7.81 (dt, *J*=8.6, 1.8, 1H), 7.46 (d, *J*=8.9, 1H), 7.18 – 7.13 (m, 1H), 7.08 – 6.98 (m, 2H), 6.33 (qd, *J*=6.4, 3.3, 1H), 5.08 (t, *J*=8.4, 2H), 4.57 (s, 2H), 4.30 – 4.24 (m, 1H), 3.70 (d, *J*=4.1, 3H), 3.13 (ddq, *J*=23.7, 12.0, 6.6, 1H), 1.84 – 1.72 (m, 0H), 1.86 – 1.54 (m, 3H), 1.51 (s, 10H), 1.44 (d, *J*=4.9, 9H), 1.40 – 1.22 (m, 3H). **¹³C NMR (101 MHz, CDCl$_3$) δ** = 173.29, 168.21, 155.43, 154.79, 154.30, 150.89, 146.62, 140.13, 135.36, 129.28, 125.50, 124.14, 123.08, 115.21, 112.14, 105.11, 104.98, 82.49, 80.00, 68.55, 66.67, 53.14, 52.37, 40.72, 32.53, 29.27, 28.39, 28.14, 22.50, 22.34.

Compound 34

Compound **16** (0.045 mmol, 0.020 g) was dissolved in DMF (1 mL). Boc-Lys-OMe.HOAc (0.076 mmol, 0.020 g) and DiPEA (0.135 mmol, 24 μL) were added and the mixture was stirred for 16 h at r.t.. TLC analysis indicated complete conversion of the starting material (5% MeOH in DCM, R$_f$=0.8). The reaction mixture was poured in 0.1M HCl (aq.) and washed with DCM (3x). The combined organic layers were washed with a saturated solution of NaHCO$_3$ (aq.) (3x), dried (MgSO$_4$) and concentrated *in vacuo*. Purification with silica gel column chromatography (DCM → 0.5% MeOH in DCM) yielded compound **34** (0.035 mmol, 0.020 g, 78%). **¹H NMR (300 MHz, DMSO-*d$_6$*) δ** = 8.14 – 8.02 (m, 2H), 7.87 (dt, *J*=8.7, 1.5, 1H), 7.66 (d, *J*=7.7, 1H), 7.59 (d, *J*=8.2, 1H), 7.45 – 7.15 (m, 4H), 6.42 – 6.31 (m, 1H), 5.06 (d, *J*=8.4, 1H), 4.99 (s, 1H), 4.28 (d, *J*=5.6, 1H), 3.72 (d, *J*=3.3, 3H), 3.15 (tt, *J*=13.5, 6.8, 2H), 1.71 (d, *J*=6.5, 3H), 1.68 – 1.50 (m, 1H), 1.46 (d, *J*=3.6, 10H), 1.27 (s, 5H), 0.95 – 0.82 (m, 2H).

Compound 35

Compound **36** (0.2 mmol, 0.040 g) was dissolved in AcN (1 mL). Boc-Lys-OMe.HOAc (0.3 mmol, 0.08 g), N,N'-disuccinimidyl carbonate (0.4 mmol, 102 mg) and DiPEA (0.50 mmol, 86 µL) were added and the mixture was stirred for 1 h at r.t.. TLC analysis indicated complete conversion of the starting material (5% MeOH in DCM, R_f=0.5). The reaction mixture was poured in 0.1M HCl (aq.) and washed with DCM (3x). The combined organic layers were washed with a saturated solution of $NaHCO_3$ (aq.) (3x), dried ($MgSO_4$) and concentrated *in vacuo*. Purification with silica gel column chromatography (DCM → 0.5% MeOH in DCM) yielded compound **43** (0.15 mmol, 0.070 g, 75%). **^{1}H NMR (400 MHz, CDCl$_3$)** δ 7.62 (s, 1H), 7.00 (s, 1H), 6.14 (s, 2H), 5.45 (s, 2H), 5.18 (d, *J* = 9.0 Hz, 2H), 4.30 (d, *J* = 4.8 Hz, 1H), 3.75 (s, 4H), 3.22 (dd, *J* = 12.9, 6.7 Hz, 3H), 1.90 – 1.76 (m, 2H), 1.71 – 1.51 (m, 4H), 1.48 – 1.32 (m, 14H). **^{13}C NMR (101 MHz, CDCl$_3$)** δ 173.27, 155.85, 155.53, 152.52, 147.22, 131.18, 107.28, 105.71, 103.16, 79.95, 63.40, 53.14, 52.33, 40.75, 32.40, 29.24, 28.31, 22.43.

Compound 36
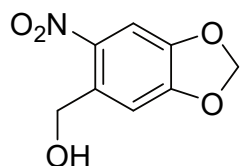
6-nitropiperonal (10 mmol, 1.95 g) was dissolved in EtOH (15 mL) and cooled down to 0°C. NaBH$_4$ (12 mmol, 0.46 g) was added and the mixture was allowed to stir for 1 hour at 0°C. TLC analysis (20% EtOAc in Pnt, R_f=0.2) indicated complete conversion of the starting material. A saturated solution of NH$_4$Cl (aq.) was added extremely carefully to quench leftover reagents. The mixture was diluted with H$_2$O and consequently extracted with DCM (3x). The organic layers were combined, dried (MgSO$_4$) and concentrated *in vacuo* to afford compound **36** (9.64 mmol, 1.90 g) in a 96% yield.

References

(1)   Maurits, E.; van de Graaff, M. J.; Maiorana, S.; Wander, D. P. A.; Dekker, P. M.; van der Zanden, S. Y.; Florea, B. I.; Neefjes, J. J. C.; Overkleeft, H. S.; van Kasteren, S. I. Immunoproteasome Inhibitor–Doxorubicin Conjugates Target Multiple Myeloma Cells and Release Doxorubicin upon Low-Dose Photon Irradiation. *J. Am. Chem. Soc.* **2020**, *142* (16), 7250–7253.

(2)   Barltrop, J. A.; Plant, P. J.; Schofield, P. Photosensitive Protective Groups. *Chem. Commun. Lond.* **1966**, No. 22, 822.

(3)   Holmes, C. P.; Jones, D. G. Reagents for Combinatorial Organic Synthesis: Development of a New o-Nitrobenzyl Photolabile Linker for Solid Phase Synthesis. *J. Org. Chem.* **1995**, *60* (8), 2318–2319.

(4)   Photolabile Protecting Groups and Linkers. *J. Chem. Soc. Perkin 1* **2002**, No. 2, 125–142.

(5)   Deshpande, R. K.; Waterhouse, G. I. N.; Jameson, G. B.; Telfer, S. G. Photolabile Protecting Groups in Metal–Organic Frameworks: Preventing Interpenetration and Masking Functional Groups. *Chem Commun* **2012**, *48* (10), 1574–1576.

(6)   Klán, P.; Šolomek, T.; Bochet, C. G.; Blanc, A.; Givens, R.; Rubina, M.; Popik, V.; Kostikov, A.; Wirz, J. Photoremovable Protecting Groups in Chemistry and Biology: Reaction Mechanisms and Efficacy. *Chem. Rev.* **2013**, *113* (1), 119–191.

(7)   Šolomek, T.; Mercier, S.; Bally, T.; Bochet, C. G. Photolysis of Ortho-Nitrobenzylic Derivatives: The Importance of the Leaving Group. *Photochem. Photobiol. Sci.* **2012**, *11* (3), 548.

(8)   Rodenko, B.; Toebes, M.; Hadrup, S. R.; van Esch, W. J. E.; Molenaar, A. M.; Schumacher, T. N. M.; Ovaa, H. Generation of Peptide–MHC Class I Complexes through UV-Mediated Ligand Exchange. *Nat. Protoc.* **2006**, *1* (3), 1120–1132.

(9)   Kaplan, J. H.; Forbush, B.; Hoffman, J. F. Rapid Photolytic Release of Adenosine 5'-Triphosphate from a Protected Analogue: Utilization by the Na:K Pump of Human Red Blood Cell Ghosts? *Biochemistry* **1978**, *17* (10), 1929–1935.

(10)   Hasan, A.; Stengele, K.-P.; Giegrich, H.; Cornwell, P.; Isham, K. R.; Sachleben, R. A.; Pfleiderer, W.; Foote, R. S. Photolabile Protecting Groups for Nucleosides: Synthesis and Photodeprotection Rates. *Tetrahedron* **1997**, *53* (12), 4247–4264.

(11)   Engels, J.; Schlaeger, E. J. Synthesis, Structure, and Reactivity of Adenosine Cyclic 3',5'-Phosphate-Benzyltriesters. *J. Med. Chem.* **1977**, *20* (7), 907–911.

(12)   Patterson, D. M.; Nazarova, L. A.; Prescher, J. A. Finding the Right (Bioorthogonal) Chemistry. *ACS Chem. Biol.* **2014**, *9* (3), 592–605.

(13)   Richards, N. G. J.; Cory, M. Computational Methods in the Design of Photocaged Compounds. I. Spectroscopic Calculations upon Substituted Isochromenes. *Int. J. Quantum Chem.* **1992**, *44* (S19), 65–76.

(14)   Silva, J. M.; Silva, E.; Reis, R. L. Light-Triggered Release of Photocaged Therapeutics - Where Are We Now? *J. Controlled Release* **2019**, *298*, 154–176.

(15)   Givens, R. S.; Matuszewski, B.; Athey, P. S.; Stoner, M. R. Photochemistry of Phosphate Esters: An Efficient Method for the Generation of Electrophiles. *J. Am. Chem. Soc.* **1990**, *112* (16), 6016–6021.

(16)   Umeda, N.; Takahashi, H.; Kamiya, M.; Ueno, T.; Komatsu, T.; Terai, T.; Hanaoka, K.; Nagano, T.; Urano, Y. Boron Dipyrromethene As a Fluorescent Caging Group for Single-

Photon Uncaging with Long-Wavelength Visible Light. *ACS Chem. Biol.* **2014**, *9* (10), 2242–2246.

(17)   Sheehan, J. C.; Umezawa, K. Phenacyl Photosensitive Blocking Groups. *J. Org. Chem.* **1973**, *38* (21), 3771–3774.

(18)   Zayat, L.; Calero, C.; Alborés, P.; Baraldo, L.; Etchenique, R. A New Strategy for Neurochemical Photodelivery: Metal–Ligand Heterolytic Cleavage. *J. Am. Chem. Soc.* **2003**, *125* (4), 882–883.

(19)   Wagner, N.; Schuhmacher, M.; Lohmann, A.; Nadler, A. A Coumarin Triflate Reagent Enables One-Step Synthesis of Photo-Caged Lipid Metabolites for Studying Cell Signaling. *Chem. – Eur. J.* **2019**, *25* (68), 15483–15487.

(20)   Bier, C.; Binder, D.; Drobietz, D.; Loeschcke, A.; Drepper, T.; Jaeger, K.-E.; Pietruszka, J. Photocaged Carbohydrates: Versatile Tools for Controlling Gene Expression by Light. *Synthesis* **2016**, *49* (01), 42–52.

(21)   Courtney, T.; Deiters, A. Recent Advances in the Optical Control of Protein Function through Genetic Code Expansion. *Curr. Opin. Chem. Biol.* **2018**, *46*, 99–107.

(22)   Ruble, B. K.; Yeldell, S. B.; Dmochowski, I. J. Caged Oligonucleotides for Studying Biological Systems. *J. Inorg. Biochem.* **2015**, *150*, 182–188.

(23)   Liu, Q.; Deiters, A. Optochemical Control of Deoxyoligonucleotide Function via a Nucleobase-Caging Approach. *Acc. Chem. Res.* **2014**, *47* (1), 45–55. https://doi.org/10.1021/ar400036a.

(24)   Lee, H.-M.; Larson, D. R.; Lawrence, D. S. Illuminating the Chemistry of Life: Design, Synthesis, and Applications of "Caged" and Related Photoresponsive Compounds. *ACS Chem. Biol.* **2009**, *4* (6), 409–427.

(25)   Amatrudo, J. M.; Olson, J. P.; Agarwal, H. K.; Ellis-Davies, G. C. R. Caged Compounds for Multichromic Optical Interrogation of Neural Systems. *Eur. J. Neurosci.* **2015**, *41* (1), 5–16.

(26)   Piggott, A. M.; Karuso, P. Synthesis of a New Hydrophilic O-Nitrobenzyl Photocleavable Linker Suitable for Use in Chemical Proteomics. *Tetrahedron Lett.* **2005**, *46* (47), 8241–8244.

(27)   Sinha, R. P.; Häder, D.-P. UV-Induced DNA Damage and Repair: A Review. *Photochem. Photobiol. Sci.* **2002**, *1* (4), 225–236.

(28)   Ryu, K. A.; Stutts, L.; Tom, J. K.; Mancini, R. J.; Esser-Kahn, A. P. Stimulation of Innate Immune Cells by Light-Activated TLR7/8 Agonists. *J. Am. Chem. Soc.* **2014**, *136* (31), 10823–10825.

(29)   Björn, L. O. Light as a Tool for Biologists: Recent Developments. In *Photobiology*; Björn, L. O., Ed.; Springer New York: New York, NY, **2015**; 51–70.

(30)   Hogenkamp, F.; Hilgers, F.; Knapp, A.; Klaus, O.; Bier, C.; Binder, D.; Jaeger, K.; Drepper, T.; Pietruszka, J. Effect of Photocaged Isopropyl β- D -1-thiogalactopyranoside Solubility on the Light Responsiveness of LacI-controlled Expression Systems in Different Bacteria. *ChemBioChem* **2021**, *22* (3), 539–547.

(31)   Lusic, H.; Deiters, A. A New Photocaging Group for Aromatic N-Heterocycles. *N. Y.* **2006**, No. 13, 4.

(32)   Berroy, P.; Viriot, M. L.; Carré, M. C. Photolabile Group for 5H-OH Protection of Nucleosides: Synthesis and Photodeprotection Rate. **2001**, 4.

(33)   Momotake, A.; Lindegger, N.; Niggli, E.; Barsotti, R. J.; Ellis-Davies, G. C. R. The Nitrodibenzofuran Chromophore: A New Caging Group for Ultra-Efficient Photolysis in Living Cells. *Nat. Methods* **2006**, *3* (1), 35–40.

(34)   Komori, N.; Jakkampudi, S.; Motoishi, R.; Abe, M.; Kamada, K.; Furukawa, K.; Katan, C.; Sawada, W.; Takahashi, N.; Kasai, H.; Xue, B.; Kobayashi, T. Design and Synthesis of a New Chromophore, 2-(4-Nitrophenyl)Benzofuran, for Two-Photon Uncaging Using near-IR Light. *Chem. Commun.* **2016**, *52* (2), 331–334.

(35)   Bashkatov, A. N.; Genina, E. A.; Kochubey, V. I.; Tuchin, V. V. Optical Properties of Human Skin, Subcutaneous and Mucous Tissues in the Wavelength Range from 400 to 2000 Nm. *J. Phys. Appl. Phys.* **2005**, *38* (15), 2543–2555.

(36)   Andrasfalvy, B. K.; Zemelman, B. V.; Tang, J.; Vaziri, A. Two-Photon Single-Cell Optogenetic Control of Neuronal Activity by Sculpted Light. *Proc. Natl. Acad. Sci.* **2010**, *107* (26), 11981–11986.

(37)   Brown, E. B.; Shear, J. B.; Adams, S. R.; Tsien, R. Y.; Webb, W. W. Photolysis of Caged Calcium in Femtoliter Volumes Using Two-Photon Excitation. *Biophys. J.* **1999**, *76* (1), 489–499.

(38)   Rumi, M.; Perry, J. W. Two-Photon Absorption: An Overview of Measurements and Principles. *Adv. Opt. Photonics* **2010**, *2* (4), 451.

(39)   Gential, G. P. P.; Hogervorst, T. P.; Tondini, E.; van de Graaff, M. J.; Overkleeft, H. S.; Codée, J. D. C.; van der Marel, G. A.; Ossendorp, F.; Filippov, D. V. Peptides Conjugated to 2-Alkoxy-8-Oxo-Adenine as Potential Synthetic Vaccines Triggering TLR7. *Bioorg. Med. Chem. Lett.* **2019**, *29* (11), 1340–1344.

(40)   Teague, S. J. Facile Synthesis of a O-Nitrobenzyl Photolabile Linker for Combinatorial Chemistry. *Tetrahedron Lett.* **1996**, *37* (32), 5751–5754.

(41)   Tonga, M. Tunable Optical Properties of Push-Pull Chromophores: End Group Effect. *Tetrahedron Lett.* **2020**, *61* (32), 152205.

(42)   Barker, P.; Finke, P.; Thompson, K. Preparation and Cyclization of Aryloxyacetaldehyde Acetals; A General Synthesis of 2,3-Unsubstituted Benzofurans. *Synth. Commun.* **1989**, *19* (1–2), 257–265.

(43)   Morales, A. R.; Frazer, A.; Woodward, A. W.; Ahn-White, H.-Y.; Fonari, A.; Tongwa, P.; Timofeeva, T.; Belfield, K. D. Design, Synthesis, and Structural and Spectroscopic Studies of Push–Pull Two-Photon Absorbing Chromophores with Acceptor Groups of Varying Strength. *J. Org. Chem.* **2013**, *78* (3), 1014–1025.

(44)   Kosak, T. M.; Conrad, H. A.; Korich, A. L.; Lord, R. L. Ether Cleavage Re-Investigated: Elucidating the Mechanism of BBr $_3$ -Facilitated Demethylation of Aryl Methyl Ethers: Ether Cleavage Re-Investigated. *Eur. J. Org. Chem.* **2015**, *2015* (34), 7460–7467.